Journal of the Physical Society of Japan **94**, 094706 (2025) **Full Papers**
https://doi.org/10.7566/JPSJ.94.094706

Onsager Reciprocal Relations for Charge and Spin Transport in Periodically Driven Systems

Naoya Arakawa[1*] and Kenji Yonemitsu[1,2]

[1]*The Institute of Science and Engineering, Chuo University, Bunkyo, Tokyo 112-8551, Japan*
[2]*Department of Physics, Chuo University, Bunkyo, Tokyo 112-8551, Japan*

(Received April 10, 2025; accepted July 4, 2025; published online August 19, 2025)

A time-periodic driving field can be used to generate and control transport phenomena. Any transport coefficients in the linear-response regime are restricted by the Onsager reciprocal relations, but these relations in periodically driven systems have been poorly understood. In particular, the Onsager reciprocal relation in spin transport of periodically driven systems is lacking despite the fact that it guarantees the detection of a spin current via the inverse spin Hall effect. Here we establish the Onsager reciprocal relations for charge and spin transport in periodically driven systems. We consider the time-averaged charge and spin off-diagonal dc conductivities σ_{yx}^{C} and σ_{yx}^{S}, which are the transport coefficients for the charge and spin currents, respectively, perpendicular to the probe electric field in the nonequilibrium steady state with the pump field of light. First, we argue the Onsager reciprocal relations for these conductivities with the pump field of circularly, linearly, or bicircularly polarized light. We show that σ_{yx}^{C} and σ_{yx}^{S} satisfy the Onsager reciprocal relations in all the cases considered, but their main terms depend on the polarization of light. In the case with circularly or linearly polarized light, σ_{yx}^{C} is restricted to the antisymmetric or symmetric part, respectively, whereas σ_{yx}^{S} is restricted to the antisymmetric part. Meanwhile, in the case with bicircularly polarized light, σ_{yx}^{C} and σ_{yx}^{S} are not restricted to either the antisymmetric or symmetric parts generally. Then, we numerically study the Onsager reciprocal relations for σ_{yx}^{C} and σ_{yx}^{S} in periodically driven Sr_2RuO_4 using the Floquet linear-response theory. Our numerical calculations validate our general arguments. Therefore, the spin current generated in periodically driven systems is detectable by the inverse spin Hall effect. Our numerical calculations also show that σ_{yx}^{C} cannot necessarily be regarded as the anomalous Hall conductivity even with broken time-reversal symmetry, whereas σ_{yx}^{S} can be regarded as the spin Hall conductivity in all the cases considered. Our results suggest that it is highly required to check whether or not the charge and spin off-diagonal conductivities are dominated by the antisymmetric parts in discussing the anomalous Hall and spin Hall effects, respectively. This study will become a cornerstone of theoretical and experimental studies of transport phenomena in periodically driven systems.

1. Introduction

Periodically driven systems have opened a new way for light-induced and light-controlled transport phenomena. In general, systems are periodically driven by a time-periodic field such as the pump field of light. Because of the time periodicity, the periodically driven systems are described by the Floquet Hamiltonian.[1,2] Since this Hamiltonian can be tuned by varying the parameters of the pump field, various properties of the systems can be engineered without changing the materials. This is called Floquet engineering.[3–6] For example, the pump field of circularly polarized light (CPL) can be used to induce the anomalous Hall effect (AHE),[7–11] in which the charge current perpendicular to the probe field is generated.[12–14] Furthermore, the charge current generated in this AHE can be changed in magnitude and direction by varying the amplitude and helicity of CPL.[7,8,10,11] Such optical control is also possible for the spin Hall effect (SHE),[11,15] in which the spin current, the flow of the spin angular momentum, is generated with the probe field perpendicular to it.[16–18]

Despite various studies of transport phenomena in periodically driven systems, the Onsager reciprocal relations in these systems have been poorly understood. In general, the Onsager reciprocal relations connect two transport coefficients.[19–21] Therefore, these relations provide general constraints on the symmetry of transport coefficients. Such constraints are useful for theoretical and experimental studies of transport phenomena. Moreover, the Onsager reciprocal relations are extremely important for spin transport. In general, it is much harder to detect the spin current than the charge current. Because of this, the spin current is usually detected indirectly in experiments. In fact, the observation of the inverse SHE can be regarded as the existence of the SHE[22,23] because their transport coefficients are connected by the Onsager reciprocal relation; in the inverse SHE, the charge current perpendicular to the spin current is generated.[22,23] Although there are some studies of the Onsager reciprocal relations in periodically driven systems,[24–27] that relation for spin transport has been unexplored yet.

In this paper, we theoretically study the Onsager reciprocal relations for charge and spin transport in periodically driven systems. The main results are summarized in Table I. We consider the time-averaged charge and spin off-diagonal dc conductivities σ_{yx}^{C} and σ_{yx}^{S} to describe the charge and spin currents, respectively, perpendicular to the probe electric field in the linear-response regime for the nonequilibrium steady state of an electron system driven by the pump field of light. Figure 1 shows the set-up for their measurements. We begin with general arguments about the Onsager reciprocal relations for σ_{yx}^{C} and σ_{yx}^{S} in the systems driven by CPL, linearly polarized light (LPL), or bicircularly polarized light (BCPL). Here BCPL consists of a linear combination of the left- and right-handed CPL with different frequencies Ω and $\beta\Omega$ and a relative phase difference θ[28–30] (see Fig. 2). We show that σ_{yx}^{C} and σ_{yx}^{S} satisfy the Onsager reciprocal relations in all the cases considered, although their main terms depend on the polarization of light. In the case with CPL or LPL, the main term of σ_{yx}^{C} is given by the antisymmetric or symmetric part, respectively, whereas that of σ_{yx}^{S} is given by the

Table I. The Onsager reciprocal relations for $\sigma^{\rm C}_{yx}$ and $\sigma^{\rm S}_{yx}$ in the nonequilibrium steady states of systems driven by CPL, LPL, and BCPL. $\sigma^{\rm C}_{yx}$ and $\sigma^{\rm S}_{yx}$ are the transport coefficients for the charge and spin currents, respectively, along the y axis perpendicular to the probe electric field applied along the x axis with the pump field $\mathbf{A}_{\rm pump}(t)$; $\sigma^{\rm C}_{xy}$ and $\tilde{\sigma}^{\rm S}_{xy}$ are those for the charge currents along the x axis perpendicular to the probe electric and spin fields, respectively, along the y axis with $\mathbf{A}_{\rm pump}(t)$; and $\bar{\sigma}^{\rm C}_{xy}$ and $\bar{\tilde{\sigma}}^{\rm S}_{xy}$ are those for the charge currents along the x axis perpendicular to the probe electric and spin fields, respectively, along the y axis with $\mathbf{A}_{\rm pump}(-t)$. In the case with CPL or LPL, $\sigma^{\rm C}_{yx}$ is restricted to the antisymmetric part $(\sigma^{\rm C}_{yx}-\sigma^{\rm C}_{xy})/2$ (corresponding to the anomalous Hall conductivity) or the symmetric part $(\sigma^{\rm C}_{yx}+\sigma^{\rm C}_{xy})/2$, respectively, whereas $\sigma^{\rm S}_{yx}$ is restricted to the antisymmetric part $(\sigma^{\rm S}_{yx}-\tilde{\sigma}^{\rm S}_{xy})/2$ (corresponding to the spin Hall conductivity). (For the reason why we have defined the antisymmetric part of $\sigma^{\rm S}_{yx}$ in this way, read the last paragraph of Sect. 2.2.1.) Meanwhile, in the case with BCPL, $\sigma^{\rm C}_{yx}$ and $\sigma^{\rm S}_{yx}$ are restricted to neither the antisymmetric nor symmetric parts generally.

	CPL	LPL	BCPL
$\sigma^{\rm C}_{yx}$	$\sigma^{\rm C}_{yx}=-\sigma^{\rm C}_{xy}$	$\sigma^{\rm C}_{yx}=\sigma^{\rm C}_{xy}$	$\sigma^{\rm C}_{yx}=\bar{\sigma}^{\rm C}_{xy}$
$\sigma^{\rm S}_{yx}$	$\sigma^{\rm S}_{yx}=-\tilde{\sigma}^{\rm S}_{xy}$	$\sigma^{\rm S}_{yx}=-\bar{\tilde{\sigma}}^{\rm S}_{xy}$	$\sigma^{\rm S}_{yx}=-\bar{\tilde{\sigma}}^{\rm S}_{xy}$

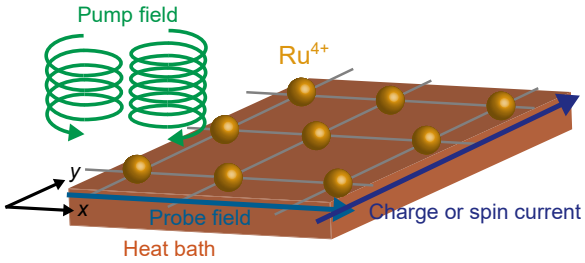

Fig. 1. (Color online) The setup for the pump-probe measurements of $\sigma^{\rm C}_{yx}$ and $\sigma^{\rm S}_{yx}$ in our periodically driven systems. $\sigma^{\rm C}_{yx}$ and $\sigma^{\rm S}_{yx}$ are the transport coefficients for describing the charge and spin currents, respectively, along the y axis, which are perpendicular to the probe field applied along the x axis in the nonequilibrium steady state with the pump field. The system is periodically driven Sr_2RuO_4 and is coupled to the heat bath. In Sr_2RuO_4, Ru^{4+} ions form the square lattice. This panel shows the case with the pump field of BCPL; the cases with those of CPL and LPL are also considered.

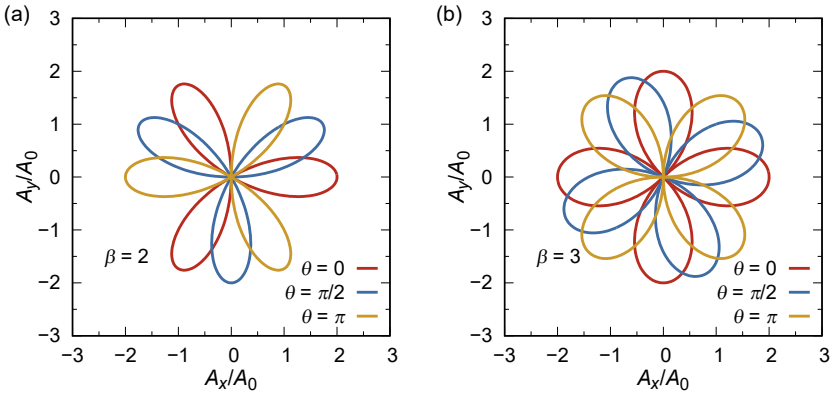

Fig. 2. (Color online) The trajectories of the pump field of BCPL at (a) $\beta=2$ and (b) $\beta=3$ and $\theta=0$, $\frac{\pi}{2}$, or π. The three or four loops with the same color are obtained per period of the pump field at $\beta=2$ or 3, respectively.

antisymmetric part. This suggests that the antisymmetric part of $\sigma^{\rm S}_{yx}$ can be finite even with time-reversal symmetry, whereas that of $\sigma^{\rm C}_{yx}$ is finite only without it. This difference arises from the difference between the time-reversal symmetries of the charge and spin currents. Meanwhile, in the case with BCPL, the Onsager reciprocal relations do not restrict $\sigma^{\rm C}_{yx}$ and $\sigma^{\rm S}_{yx}$ to either the antisymmetric or symmetric parts generally. This unusual property is due to the lack of a simple relation between the pump field of BCPL and its time-reversal counterpart. Then, we numerically test the Onsager reciprocal relations for $\sigma^{\rm C}_{yx}$ and $\sigma^{\rm S}_{yx}$ by applying the Floquet linear-response theory[11] to a model of Sr_2RuO_4 driven by CPL, LPL, or BCPL with weak coupling to a heat bath. We demonstrate the validity of our arguments. Therefore, our results indicate that, even for periodically driven systems, the spin current can be detected by the inverse SHE. This is useful to develop and observe many spintronics phenomena in periodically driven systems. Then, our numerical calculations with BCPL show that the main term of $\sigma^{\rm S}_{yx}$ is given by the antisymmetric part. Combining these results with the results with CPL or LPL, we conclude that $\sigma^{\rm S}_{yx}$ can be regarded as the spin Hall conductivity in all the cases considered. Our numerical calculations with BCPL also show that the main term of $\sigma^{\rm C}_{yx}$ depends on the magnitude, β, and θ of the pump field. More precisely, $\sigma^{\rm C}_{yx}$ with BCPL for weak magnitude is dominated by the antisymmetric part, whereas that for moderately strong magnitude is almost vanishing in the cases of $(\beta,\theta)=(2,0)$, $(2,\frac{\pi}{2})$, $(2,\pi)$, $(3,0)$, and $(3,\pi)$ or dominated by the symmetric part in the cases of $(\beta,\theta)=(2,\frac{\pi}{4})$, $(2,\frac{3\pi}{4})$, $(3,\frac{\pi}{4})$, $(3,\frac{\pi}{2})$, and $(3,\frac{3\pi}{4})$. Therefore, $\sigma^{\rm C}_{yx}$ cannot necessarily be regarded as the anomalous Hall conductivity even with broken time-reversal symmetry. Our results suggest that it is necessary to check the main terms of $\sigma^{\rm C}_{yx}$ and $\sigma^{\rm S}_{yx}$ in discussing the AHE and SHE, respectively.

The remainder of this paper is organized as follows. In Sect. 2, we argue the Onsager reciprocal relations in nondriven and periodically driven systems. After reviewing these relations in nondriven systems, we derive the Onsager reciprocal relations for $\sigma^{\rm C}_{yx}$ and $\sigma^{\rm S}_{yx}$ in the electron systems driven by CPL, LPL, or BCPL. In Sect. 3, we introduce the model of periodically driven Sr_2RuO_4. In this model, we consider the heat bath as well as the system of Sr_2RuO_4 driven by the pump field of light and suppose that a nonequilibrium steady state is realized due to the damping induced by the coupling to the heat bath. The reason why we choose Sr_2RuO_4 is twofold: its realistic model possesses the finite spin off-diagonal dc conductivity, which is more difficult to be realized than the finite charge off-diagonal dc conductivity; and its electronic structure is so simple that the Onsager reciprocal relations for these conductivities can be

numerically studied even in the case with BCPL. In Sect. 4, we formulate $\sigma^{\rm C}_{yx}$ and $\sigma^{\rm S}_{yx}$ as well as their counterparts appearing in the Onsager reciprocal relations using the Floquet linear-response theory. We also comment on the applicability of this theory. In Sect. 5, we show the numerical results of the Onsager reciprocal relations for $\sigma^{\rm C}_{yx}$ and $\sigma^{\rm S}_{yx}$ in Sr_2RuO_4 driven by CPL, LPL, or BCPL at $\beta = 2$ and 3. In Sect. 6, we discuss the origin of the characteristic θ dependences of $\sigma^{\rm C}_{yx}$ and $\sigma^{\rm S}_{yx}$ in the cases with BCPL, compare our results with other relevant studies, and remark on the experimental realization of our results. In Sect. 7, we make some concluding remarks on implications and outlooks.

2. Onsager Reciprocal Relations

We begin with general argument about the Onsager reciprocal relations in nondriven or periodically driven systems. We argue these relations for the charge and spin off-diagonal dc conductivities in Sects. 2.1 and 2.2, respectively. The results for periodically driven systems are summarized in Table I. Although the Onsager reciprocal relations in nondriven systems may be well known, we will review them below to help the readers understand our general arguments in periodically driven systems. Since the essential symmetry in discussing the Onsager reciprocal relations is the symmetry against a time-reversal operation,[19–21] we will not specify whether a certain vector is a vector or pseudovector.

As we will show below, the charge and spin off-diagonal dc conductivities satisfy the Onsager reciprocal relations in all the cases considered, although there are some essential differences due to the different time-reversal symmetries of the charge and spin currents (Fig. 3). The following results are valid in general as long as the probe field can be described in the linear-response theory.

2.1 *Charge off-diagonal dc conductivity*

We argue the Onsager reciprocal relations for the charge off-diagonal dc conductivity in nondriven or periodically driven systems. In the following arguments, we suppose that this conductivity is given by the correlation function between the charge current operators. This is valid as long as the probe field is of linear response.

2.1.1 *Nondriven systems*

First, we consider the nondriven case with a magnetic field $\mathbf{H}$. In general, the Onsager reciprocal relation connects the transport coefficient for a certain transport phenomenon with another for the transport phenomenon obtained by applying the time-reversal operation to the original phenomenon.[19–21] Therefore, the Onsager reciprocal relation for the charge off-diagonal dc conductivity with $\mathbf{H}$ is given by[19–21]

$$\sigma^{\rm C}_{yx}(\mathbf{H}) = (-1)^2\sigma^{\rm C}_{xy}(-\mathbf{H}), \tag{1}$$

where $\sigma^{\rm C}_{yx}(\mathbf{H})$ is the charge off-diagonal dc conductivity for the charge current $J^y_{\rm C}$ generated perpendicular to the probe electric field E_x in the presence of $\mathbf{H}$ [i.e., $J^y_{\rm C} = \sigma^{\rm C}_{yx}(\mathbf{H})E_x$], and $\sigma^{\rm C}_{xy}(-\mathbf{H})$ is that for the charge current $J^x_{\rm C}$ generated perpendicular to the probe electric field E_y in the presence of $-\mathbf{H}$ [i.e., $J^x_{\rm C} = \sigma^{\rm C}_{xy}(-\mathbf{H})E_y$]. The factor $(-1)^2$ in Eq. (1) arises from the sign changes in the charge current operators appearing in the charge off-diagonal dc conductivity under the time-reversal operation [Fig. 3(a)]. Then, we suppose that the charge off-diagonal dc conductivity satisfies $\sigma^{\rm C}_{xy}(-\mathbf{H}) = -\sigma^{\rm C}_{xy}(\mathbf{H})$, which usually holds in the case with $\mathbf{H} = (0\ 0\ H)^T$. By combining this relation with Eq. (1), the Onsager reciprocal relation can be reduced to

$$\sigma^{\rm C}_{yx}(\mathbf{H}) = -\sigma^{\rm C}_{xy}(\mathbf{H}). \tag{2}$$

This is often called the Onsager reciprocal relation, but it has been derived from a combination of the Onsager reciprocal relation Eq. (1) and the additional symmetric property [i.e., $\sigma^{\rm C}_{xy}(-\mathbf{H}) = -\sigma^{\rm C}_{xy}(\mathbf{H})$]. This point is important to discuss whether a certain transport coefficient satisfies the Onsager reciprocal relation. If there is no such additional symmetric property, whether the Onsager reciprocal relation holds should be discussed using the equation such as Eq. (1); this is true in the case with BCPL, as we will show in Sect. 2.1.2.

Next, we consider the nondriven case with magnetization $\mathbf{M}$. Since $\mathbf{M}$ breaks time-reversal symmetry (as $\mathbf{H}$ does), the similar argument is applicable to this case; as a result, we have

$$\sigma^{\rm C}_{yx}(\mathbf{M}) = (-1)^2\sigma^{\rm C}_{xy}(-\mathbf{M}) = -\sigma^{\rm C}_{xy}(\mathbf{M}). \tag{3}$$

In driving this equation, we have supposed that $\sigma^{\rm C}_{xy}(-\mathbf{M}) = -\sigma^{\rm C}_{xy}(\mathbf{M})$ is satisfied.

In both cases, the charge off-diagonal dc conductivity has only the antisymmetric part $(\sigma^{\rm C}_{yx} - \sigma^{\rm C}_{xy})/2$ and thus can be regarded as the Hall conductivity, which is described by the antisymmetric part. This antisymmetric part can be finite only with broken time-reversal symmetry.[19]

2.1.2 *Periodically driven systems*

We now argue the Onsager reciprocal relations in periodically driven systems in two dimensions. To do this, we consider the nonequilibrium steady state under the pump field $\mathbf{A}_{\rm pump}(t)$ with a time period $T_{\rm p}$ [i.e., $\mathbf{A}_{\rm pump}(t + T_{\rm p}) = \mathbf{A}_{\rm pump}(t)$] and discuss the symmetric properties of the time-averaged charge off-diagonal dc conductivity [for its definition, see Eq. (51) for Q = C with Eq. (52)]. The

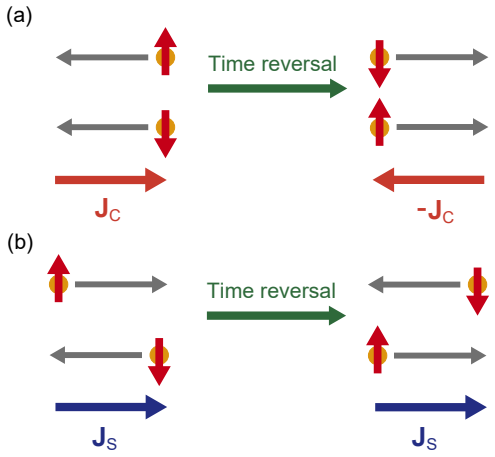

Fig. 3. (Color online) The changes in (a) the charge current $\mathbf{J}_{\rm C}$ and (b) the spin current $\mathbf{J}_{\rm S}$ under the time-reversal operation. The up or down arrows represent the spin-up or spin-down electrons, respectively. Here $\mathbf{J}_{\rm C}$ and $\mathbf{J}_{\rm S}$ are defined as $\mathbf{J}_{\rm C} = (-e)(\mathbf{J}_\uparrow + \mathbf{J}_\downarrow)$ and $\mathbf{J}_{\rm S} = (\hbar/2)(\mathbf{J}_\uparrow - \mathbf{J}_\downarrow)$, where $\mathbf{J}_\uparrow$ and $\mathbf{J}_\downarrow$ are the currents of the spin-up and spin-down electrons, respectively. Under the time-reversal operation, $\mathbf{J}_\uparrow \to -\mathbf{J}_\downarrow$ and $\mathbf{J}_\downarrow \to -\mathbf{J}_\uparrow$, resulting in $\mathbf{J}_{\rm C} \to -\mathbf{J}_{\rm C}$ and $\mathbf{J}_{\rm S} \to \mathbf{J}_{\rm S}$.

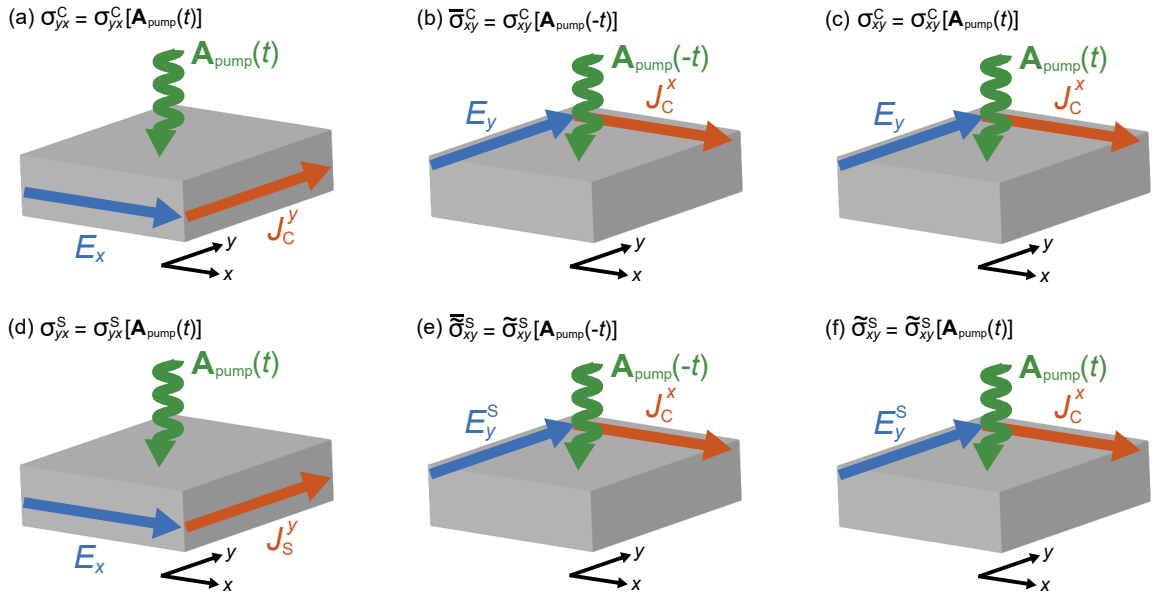

Fig. 4. (Color online) The transport phenomena described by (a) $\sigma^{C}_{yx} = \sigma^{C}_{yx}[\mathbf{A}_{pump}(t)]$, (b) $\tilde{\sigma}^{C}_{xy} = \sigma^{C}_{xy}[\mathbf{A}_{pump}(-t)]$, (c) $\sigma^{C}_{xy} = \sigma^{C}_{xy}[\mathbf{A}_{pump}(t)]$, (d) $\sigma^{S}_{yx} = \sigma^{S}_{yx}[\mathbf{A}_{pump}(t)]$, (e) $\tilde{\sigma}^{S}_{xy} = \tilde{\sigma}^{S}_{xy}[\mathbf{A}_{pump}(-t)]$, and (f) $\tilde{\sigma}^{S}_{xy} = \tilde{\sigma}^{S}_{xy}[\mathbf{A}_{pump}(t)]$. The blue arrows represent the probe electric fields E_x and E_y and the probe spin field E^S_y. Here E^S_y is given by, for example, the gradient of either the Zeeman field or a spin-dependent chemical potential; it can induce a spin current as the probe electric field can induce a charge current. The orange arrows represent the charge currents J^y_C and J^x_C and the spin current J^y_S. The green arrows represent the pump fields $\mathbf{A}_{pump}(t)$ and $\mathbf{A}_{pump}(-t)$. The x and y axes are also drawn in these panels.

following arguments can be extended to any other periodically driven systems.

First, we discuss the Onsager reciprocal relation with the pump field of left-handed CPL, $\mathbf{A}_{LCPL}(t)$, where

$$\mathbf{A}_{LCPL}(t) = (A_0 \cos \Omega t \; A_0 \sin \Omega t)^T, \tag{4}$$

and $\Omega = 2\pi/T_p$ is the light frequency. In this case, the Onsager reciprocal relation is given by

$$\sigma^{C}_{yx}[\mathbf{A}_{LCPL}(t)] = (-1)^2 \sigma^{C}_{xy}[\mathbf{A}_{LCPL}(-t)], \tag{5}$$

where $\sigma^{C}_{\nu\eta}[\mathbf{A}_{pump}(t)]$ is the time-averaged charge off-diagonal dc conductivity for the charge current J^{ν}_C generated perpendicular to the probe field E_η with $\mathbf{A}_{pump}(t)$ [Figs. 4(a)–4(c)]. Since $\mathbf{A}_{LCPL}(-t)$ is equal to the pump field of right-handed CPL,

$$\mathbf{A}_{RCPL}(t) = (A_0 \cos \Omega t \; -A_0 \sin \Omega t)^T, \tag{6}$$

Eq. (5) is rewritten as

$$\sigma^{C}_{yx}[\mathbf{A}_{LCPL}(t)] = \sigma^{C}_{xy}[\mathbf{A}_{RCPL}(t)]. \tag{7}$$

Furthermore, we suppose that the time-averaged charge off-diagonal dc conductivity changes its sign by switching the helicity of light,[11,27]

$$\sigma^{C}_{xy}[\mathbf{A}_{RCPL}(t)] = -\sigma^{C}_{xy}[\mathbf{A}_{LCPL}(t)]. \tag{8}$$

This property can be understood in terms of the symmetry of the charge current under the time-reversal operation, which switches the helicity of light.[11] Combining Eqs. (7) and (8), we can reduce the Onsager reciprocal relation in this case to

$$\sigma^{C}_{yx}[\mathbf{A}_{LCPL}(t)] = -\sigma^{C}_{xy}[\mathbf{A}_{LCPL}(t)]. \tag{9}$$

Therefore, the time-averaged charge off-diagonal dc conductivity with the pump field of CPL is restricted to be antisymmetric. This has been numerically confirmed in graphene driven by CPL.[27]

Meanwhile, in systems driven by LPL, the time-averaged charge off-diagonal dc conductivity is restricted to be symmetric,

$$\sigma^{C}_{yx}[\mathbf{A}_{LPL}(t)] = \sigma^{C}_{xy}[\mathbf{A}_{LPL}(t)], \tag{10}$$

where the pump field of LPL, $\mathbf{A}_{LPL}(t)$, is given by

$$\mathbf{A}_{LPL}(t) = (A_0 \cos \Omega t \; A_0 \cos \Omega t)^T. \tag{11}$$

Equation (10) has been also numerically confirmed in graphene driven by LPL.[27]

The difference between Eqs. (9) and (10) is due to the difference in time-reversal symmetry.[27] Note that CPL can break time-reversal symmetry,[31] whereas LPL does not. We will check Eqs. (9) and (10) for periodically driven Sr_2RuO_4 in Sect. 5.2.1.

The situation becomes different in the presence of the pump field of BCPL,[28–30] $\mathbf{A}_{BCPL}(t) = (A_x(t) \; A_y(t))^T$, where

$$A_x(t) = A_0[\cos \Omega t + \cos(\beta \Omega t - \theta)], \tag{12}$$

$$A_y(t) = A_0[\sin \Omega t - \sin(\beta \Omega t - \theta)]. \tag{13}$$

Figures 2(a) and 2(b) show the trajectories of $\mathbf{A}_{BCPL}(t)$ per period at $\beta = 2$ and 3, respectively. In this case, the Onsager reciprocal relation is written as

$$\sigma^{C}_{yx}[\mathbf{A}_{BCPL}(t)] = (-1)^2 \sigma^{C}_{xy}[\mathbf{A}_{BCPL}(-t)], \tag{14}$$

where $\mathbf{A}_{BCPL}(-t) = (A_x(-t) \; A_y(-t))^T$ is given by

$$A_x(-t) = A_0[\cos \Omega t + \cos(\beta \Omega t + \theta)], \tag{15}$$

$$A_y(-t) = -A_0[\sin \Omega t - \sin(\beta \Omega t + \theta)]. \tag{16}$$

Since $\mathbf{A}_{BCPL}(-t)$ and $\mathbf{A}_{BCPL}(t)$ are not connected by a simple relation such as $\mathbf{A}_{LCPL}(-t) = \mathbf{A}_{RCPL}(t)$, we cannot rewrite Eq. (14) anymore in general. Therefore, in periodically driven systems with BCPL, the time-averaged charge off-diagonal dc conductivity is restricted to neither the antisymmetric nor symmetric part generally. We will validate this property numerically in Sect. 5.2.2.

2.2 *Spin off-diagonal dc conductivity*

We argue the Onsager reciprocal relations for the spin off-diagonal dc conductivity. We suppose that this conductivity is given by the correlation function between the charge current and spin current operators. This is valid in the linear-response regime of the probe field. Note that this conductivity is different from that for describing the spin current generated by the probe spin field, which is given by the correlation function between the spin current operators.[32,33] We also suppose that the spin current remains unchanged under the time-reversal operation. Therefore, the following arguments are valid for any definition of the spin current as long as it is symmetric with respect to the time-reversal operation. This property against the time-reversal operation may be reasonable because the spin current is the flow of the spin angular momentum, such as $\mathbf{J}_{\mathrm{S}} = \frac{\hbar}{2}(\mathbf{J}_{\uparrow} - \mathbf{J}_{\downarrow})$,[11] where $\mathbf{J}_{\sigma}$ is the current of spin-σ electrons [Fig. 3(b)].

In this paper, we define the spin current as the flow of the z component of the spin angular momentum. In the following arguments, we discuss the Onsager reciprocal relations about the spin off-diagonal dc conductivities for the y component of this spin current perpendicular to the probe field applied along the x direction. Since the other components of the spin current have the same time-reversal symmetry, the following arguments can be applied to the spin off-diagonal dc conductivities for the other components. Furthermore, they can be extended to the spin off-diagonal dc conductivities for another spin current, the flow of the x or y component of the spin angular momentum. Namely, the following arguments are sufficient to clarify the Onsager reciprocal relations about the spin off-diagonal dc conductivities.

2.2.1 *Nondriven systems*

In the nondriven case with the magnetic field $\mathbf{H}$, the spin off-diagonal dc conductivity satisfies the Onsager reciprocal relation,

$$\sigma^{\mathrm{S}}_{yx}(\mathbf{H}) = (-1)\tilde{\sigma}^{\mathrm{S}}_{xy}(-\mathbf{H}), \tag{17}$$

where $\sigma^{\mathrm{S}}_{yx}(\mathbf{H})$ is the spin off-diagonal dc conductivity for the spin current J^{y}_{S} generated perpendicular to the probe electric field E_x in the presence of $\mathbf{H}$ [i.e., $J^{y}_{\mathrm{S}} = \sigma^{\mathrm{S}}_{yx}(\mathbf{H})E_x$], and $\tilde{\sigma}^{\mathrm{S}}_{xy}(-\mathbf{H})$ is another for the charge current J^{x}_{C} generated perpendicular to the probe spin field E^{S}_{y} (e.g., the gradient of the Zeeman field or of a spin-dependent chemical potential[34]) in the presence of $-\mathbf{H}$ [i.e., $J^{x}_{\mathrm{C}} = \tilde{\sigma}^{\mathrm{S}}_{xy}(-\mathbf{H})E^{\mathrm{S}}_{y}$]. The factor (-1) in Eq. (17) arises from the properties that the spin off-diagonal dc conductivity is given by the correlation function between the charge current and spin current operators and that only the charge current operator changes its sign under the time-reversal operation (Fig. 3). This minus sign has been missing in some studies.[35,36] Therefore, the violation of the Onsager reciprocal relation claimed in Ref. 36 may be due to the incorrect treatment about the difference between time-reversal symmetries of the charge and spin currents. Then, Eq. (17) shows that the counterpart connected by the Onsager reciprocal relation for $\sigma^{\mathrm{S}}_{yx}(\mathbf{H})$ is not $\sigma^{\mathrm{S}}_{xy}(-\mathbf{H})$, but $\tilde{\sigma}^{\mathrm{S}}_{xy}(-\mathbf{H})$, where $\sigma^{\mathrm{S}}_{xy}(-\mathbf{H})$ is the spin off-diagonal dc conductivity for the spin current J^{x}_{S} generated perpendicular to the probe electric field E_y in the presence of $-\mathbf{H}$ [i.e., $J^{x}_{\mathrm{S}} = \sigma^{\mathrm{S}}_{xy}(-\mathbf{H})E_y$]. This is because the transport coefficient for a certain transport phenomenon is connected by the Onsager reciprocal relation with that for the transport phenomenon obtained by applying the time-reversal operation to the original phenomenon,[19–21] as explained above.

The similar Onsager reciprocal relation holds in the nondriven case with the magnetization $\mathbf{M}$:

$$\sigma^{\mathrm{S}}_{yx}(\mathbf{M}) = (-1)\tilde{\sigma}^{\mathrm{S}}_{xy}(-\mathbf{M}). \tag{18}$$

These results are consistent with some previous studies,[34,37] although the origin of the minus sign appearing in the Onsager reciprocal relation is different.

Because of Eq. (17) or (18), the spin off-diagonal dc conductivity has the antisymmetric part $(\sigma^{\mathrm{S}}_{yx} - \tilde{\sigma}^{\mathrm{S}}_{xy})/2$ even with no magnetic field and thus can be regarded as the spin Hall conductivity. This is the most important difference between the spin and charge off-diagonal dc conductivities: the former possesses the antisymmetric part even with time-reversal symmetry, whereas the latter is restricted to the symmetric part with this symmetry. We have defined the antisymmetric part of σ^{S}_{yx} as not $(\sigma^{\mathrm{S}}_{yx} - \sigma^{\mathrm{S}}_{xy})/2$, but $(\sigma^{\mathrm{S}}_{yx} - \tilde{\sigma}^{\mathrm{S}}_{xy})/2$ because the latter corresponds to the spin Hall conductivity for describing the spin current along the y axis with the probe electric field applied along the x axis. This can be understood if we recall its expression in nondriven systems with no dissipation; in these systems, the spin Hall conductivity is expressed in terms of the spin Berry curvature the numerator of which is proportional to $\mathrm{Im}[\langle \mathbf{k}\alpha|J^{x}_{\mathrm{C}}|\mathbf{k}\beta\rangle\langle \mathbf{k}\beta|J^{y}_{\mathrm{S}}|\mathbf{k}\alpha\rangle]$, where $\langle \mathbf{k}\alpha|J^{x}_{\mathrm{C}}|\mathbf{k}\beta\rangle$ and $\langle \mathbf{k}\beta|J^{y}_{\mathrm{S}}|\mathbf{k}\alpha\rangle$ are the expectation values of the charge and spin current operators, respectively, over the states at momentum $\mathbf{k}$ for band indices α and β $(\neq \alpha)$. Note that in the linear-response theory, σ^{S}_{yx} and $\tilde{\sigma}^{\mathrm{S}}_{xy}$ are given by the correlation functions between J^{y}_{S} and J^{x}_{C}, whereas σ^{S}_{xy} is given by that between J^{x}_{S} and J^{y}_{C}. Therefore, $(\sigma^{\mathrm{S}}_{yx} - \tilde{\sigma}^{\mathrm{S}}_{xy})/2$ describes the SHE in the case of the spin current generated along the y axis. If the difference between the time-reversal symmetries of the charge and spin currents were neglected, the spin off-diagonal dc conductivity would have only the symmetric part. The above arguments show that a naive analogy with the Onsager reciprocal relation for the charge transport is incorrect to discuss the Onsager reciprocal relation for the spin transport.

2.2.2 *Periodically driven systems*

We turn to the cases of the periodically driven systems in two dimensions. In the following, we discuss the symmetric properties of the time-averaged spin off-diagonal dc conductivity in the nonequilibrium steady state under $\mathbf{A}_{\mathrm{pump}}(t)$. [For its definition, see Eq. (51) for Q = S with Eq. (52).] The arguments for any other periodically driven systems can be made in a similar way.

In the case with the pump field of left-handed CPL, the Onsager reciprocal relation for the time-averaged spin off-diagonal dc conductivity is given by

$$\sigma^{\mathrm{S}}_{yx}[\mathbf{A}_{\mathrm{LCPL}}(t)] = (-1)\tilde{\sigma}^{\mathrm{S}}_{xy}[\mathbf{A}_{\mathrm{LCPL}}(-t)], \tag{19}$$

where $\sigma^{\mathrm{S}}_{yx}[\mathbf{A}_{\mathrm{LPCL}}(t)]$ is the time-averaged spin off-diagonal dc conductivity for the spin current J^{y}_{S} generated perpendicular to the probe electric field E_x with $\mathbf{A}_{\mathrm{LCPL}}(t)$ [Fig. 4(d)], and $\tilde{\sigma}^{\mathrm{S}}_{xy}[\mathbf{A}_{\mathrm{LCPL}}(-t)]$ is another for the charge current J^{x}_{C} generated perpendicular to the probe spin field E^{S}_{y} with $\mathbf{A}_{\mathrm{LCPL}}(-t)$ [Fig. 4(e)]. Since $\mathbf{A}_{\mathrm{LCPL}}(-t) = \mathbf{A}_{\mathrm{RCPL}}(t)$, we have

$$\sigma^{\mathrm{S}}_{yx}[\mathbf{A}_{\mathrm{LCPL}}(t)] = -\tilde{\sigma}^{\mathrm{S}}_{xy}[\mathbf{A}_{\mathrm{RCPL}}(t)]. \tag{20}$$

Similarly, we have

$$\sigma^{\mathrm{S}}_{yx}[\mathbf{A}_{\mathrm{RCPL}}(t)] = -\tilde{\sigma}^{\mathrm{S}}_{xy}[\mathbf{A}_{\mathrm{LCPL}}(t)]. \tag{21}$$

In addition, the time-averaged spin off-diagonal dc conductivity is independent of the helicity of light,[11]

$$\sigma^{\mathrm{S}}_{yx}[\mathbf{A}_{\mathrm{LCPL}}(t)] = \sigma^{\mathrm{S}}_{yx}[\mathbf{A}_{\mathrm{RCPL}}(t)]. \tag{22}$$

This equation can be understood in terms of the symmetry of the spin current under the time-reversal operation.[11] Combining Eq. (22) with Eqs. (20) and (21), we obtain the Onsager reciprocal relation in this case,

$$\sigma^{\mathrm{S}}_{yx}[\mathbf{A}_{\mathrm{LCPL}}(t)] = -\tilde{\sigma}^{\mathrm{S}}_{xy}[\mathbf{A}_{\mathrm{LCPL}}(t)]. \tag{23}$$

For $\tilde{\sigma}^{\mathrm{S}}_{xy}[\mathbf{A}_{\mathrm{LCPL}}(t)]$, see Fig. 4(f).

The similar Onsager reciprocal relation is satisfied with the pump field of LPL:

$$\sigma^{\mathrm{S}}_{yx}[\mathbf{A}_{\mathrm{LPL}}(t)] = -\tilde{\sigma}^{\mathrm{S}}_{xy}[\mathbf{A}_{\mathrm{LPL}}(t)]. \tag{24}$$

Therefore, the time-averaged spin off-diagonal dc conductivity is restricted to be antisymmetric in the periodically driven system with the pump field of CPL or LPL. We will check this property numerically in Sect. 5.1.1.

In the case with the pump field of BCPL, the Onsager reciprocal relation for the time-averaged spin off-diagonal dc conductivity reads

$$\sigma^{\mathrm{S}}_{yx}[\mathbf{A}_{\mathrm{BCPL}}(t)] = -\tilde{\sigma}^{\mathrm{S}}_{xy}[\mathbf{A}_{\mathrm{BCPL}}(-t)]. \tag{25}$$

As well as Eq. (14), this equation cannot be rewritten anymore in general. However, as we will show in Sect. 5.1.2, the antisymmetric part dominates the time-averaged spin off-diagonal dc conductivity in the nonequilibrium steady states with BCPL. This is different from the result of the time-averaged charge off-diagonal dc conductivity with BCPL (see Sect. 5.2.2).

3. Model

To show the validity of our general arguments made in Sect. 2, we consider a concrete model and analyze its time-averaged spin and charge off-diagonal dc conductivities. Sections 3, 4, and 5 are devoted to this analysis.

In this section, we introduce the concrete model for periodically driven electron systems. As the concrete model, we consider a periodically driven multiorbital metal with weak coupling to a heat bath. Our model Hamiltonian consists of three parts:[11]

$$H(t) = H_{\mathrm{s}}(t) + H_{\mathrm{b}} + H_{\mathrm{sb}}, \tag{26}$$

where $H_{\mathrm{s}}(t)$ is the system Hamiltonian, H_{b} is the bath Hamiltonian, and H_{sb} is the system-bath coupling Hamiltonian. As $H_{\mathrm{s}}(t)$, we have considered the periodically driven Sr_2RuO_4 because it is suitable for achieving the finite time-averaged spin and charge off-diagonal dc conductivities.[11] In addition to $H_{\mathrm{s}}(t)$, we have considered H_{b} and H_{sb} because we suppose that our periodically driven system can reach a nonequilibrium steady state due to the coupling with the heat bath.[8,11,38] If such a relaxation mechanism is absent, a periodically driven system reaches an infinite-temperature state due to the heating of the pump field.[39,40] Hereafter, we use the unit $\hbar = k_{\mathrm{B}} = c = a_{\mathrm{NN}} = 1$, where a_{NN} is the distance between nearest-neighbor sites on a square lattice.

3.1 System Hamiltonian $H_s(t)$

$H_{\mathrm{s}}(t)$ consists of the hopping integrals between t_{2g}-orbital electrons in the presence of a light field $\mathbf{A}(t)$, the chemical potential μ, and the atomic SOC (i.e., the *LS* coupling):

$$H_{\mathrm{s}}(t) = \sum_{i,j}\sum_{a,b=d_{yz},d_{zx},d_{xy}}\sum_{\sigma=\uparrow,\downarrow}[t^{ab}_{ij}(t) - \mu\delta_{i,j}\delta_{a,b}]c^{\dagger}_{ia\sigma}c_{jb\sigma} + \sum_{i}\sum_{a,b=d_{yz},d_{zx},d_{xy}}\sum_{\sigma,\sigma'=\uparrow,\downarrow}\xi^{\sigma\sigma'}_{ab}c^{\dagger}_{ia\sigma}c_{ib\sigma'}, \tag{27}$$

where $c^{\dagger}_{ia\sigma}$ and $c_{ia\sigma}$ are the creation and annihilation operators, respectively, of an electron for orbital a and spin σ at site i, $t^{ab}_{ij}(t)$'s are the hopping integrals with the Peierls phase factor due to $\mathbf{A}(t)$,

$$t^{ab}_{ij}(t) = t^{ab}_{ij}e^{-ie(\mathbf{R}_i-\mathbf{R}_j)\cdot\mathbf{A}(t)}, \tag{28}$$

t^{ab}_{ij}'s are the hopping integrals in the nondriven system, and $\xi^{\sigma\sigma'}_{ab} = (\xi^{\sigma'\sigma}_{ba})^*$ is the coupling constant of the SOC for t_{2g}-orbital electrons, the finite components of which are given by

$$\xi^{\uparrow\uparrow}_{d_{yz}d_{zx}} = \xi^{\uparrow\downarrow}_{d_{zx}d_{xy}} = -\xi^{\uparrow\downarrow}_{d_{xy}d_{zx}} = -\xi^{\downarrow\downarrow}_{d_{yz}d_{zx}} = i\xi/2, \tag{29}$$

$$\xi^{\uparrow\downarrow}_{d_{xy}d_{yz}} = -\xi^{\uparrow\downarrow}_{d_{yz}d_{xy}} = \xi/2. \tag{30}$$

Using the Fourier transformation of the operators, we have

$$H_{\mathrm{s}}(t) = \sum_{\mathbf{k}}\sum_{a,b=d_{yz},d_{zx},d_{xy}}\sum_{\sigma,\sigma'=\uparrow,\downarrow}\bar{\epsilon}^{\sigma\sigma'}_{ab}(\mathbf{k},t)c^{\dagger}_{\mathbf{k}a\sigma}c_{\mathbf{k}b\sigma'}, \tag{31}$$

where

$$\bar{\epsilon}^{\sigma\sigma'}_{ab}(\mathbf{k},t) = [\epsilon_{ab}(\mathbf{k},t) - \mu\delta_{a,b}]\delta_{\sigma,\sigma'} + \xi^{\sigma\sigma'}_{ab}, \tag{32}$$

and

$$\epsilon_{ab}(\mathbf{k},t) = \sum_{j}t^{ab}_{ij}e^{-i[\mathbf{k}+e\mathbf{A}(t)]\cdot(\mathbf{R}_i-\mathbf{R}_j)}. \tag{33}$$

We choose the parameters of $H_{\mathrm{s}}(t)$ to reproduce the electronic structure of Sr_2RuO_4 near the Fermi level. The hopping integrals t^{ab}_{ij}'s in Eq. (28) are parametrized by t_1, t_2, t_3, t_4, and t_5;[11,41,42] the first three ones are nearest-neighbor terms, and the others are next-nearest-neighbor ones [Fig. 5(a)]. We choose their values as follows: $(t_1, t_2, t_3, t_4, t_5) = (0.675, 0.09, 0.45, 0.18, 0.03)$ (eV).[41] We also set $\xi = 0.17$ eV.[43] Then, we determine μ from the condition that the electron number per site is four; the value of μ is fixed at that determined for $\mathbf{A}(t) = \mathbf{0}$ in the analyses shown in Sect. 5. Figures 5(b) and 5(c) show the band structure and Fermi surface of our model for Sr_2RuO_4 with $\mathbf{A}(t) = \mathbf{0}$. The obtained Fermi surface is consistent with that observed experimentally in nondriven Sr_2RuO_4.[44] Note that Sr_2RuO_4 is a material with the simple electronic structure in which the spin off-diagonal dc conductivity is finite.[45,46]

3.2 Bath Hamiltonian H_b

H_{b} is the Hamiltonian for the Büttiker-type heat bath:[8,11,38,47,48]

$$H_{\mathrm{b}} = \sum_{i}\sum_{p}(\epsilon_p - \mu_{\mathrm{b}})b^{\dagger}_{ip}b_{ip}, \tag{34}$$

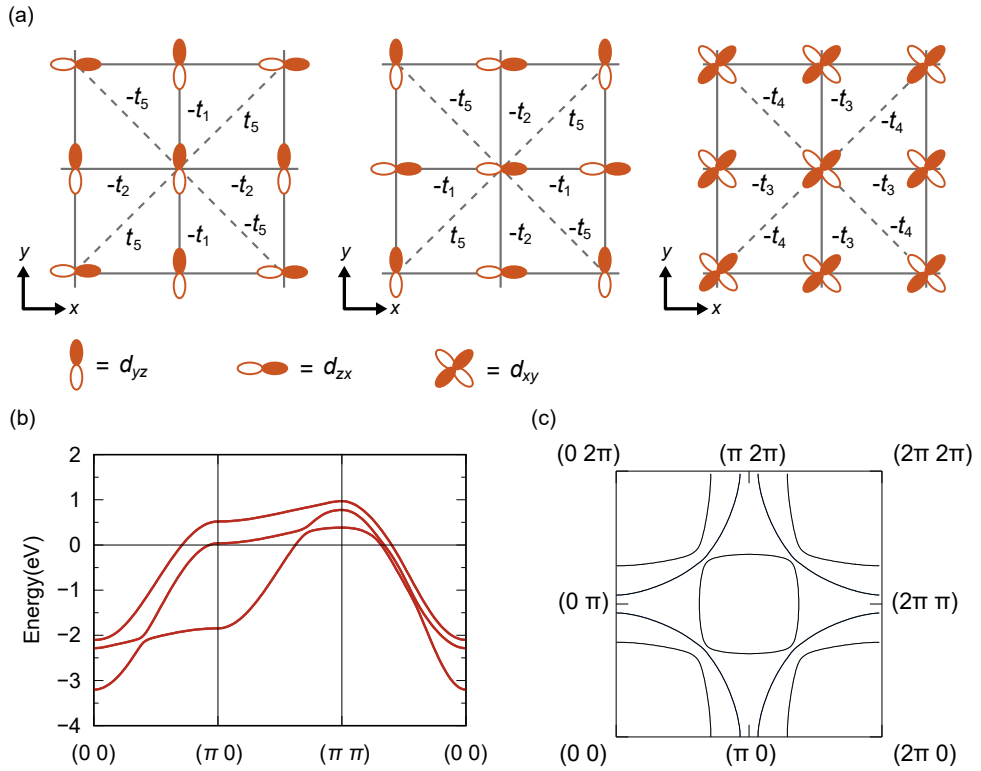

Fig. 5. (Color online) (a) The nearest neighbor and next nearest neighbor hopping integrals for the t_{2g}-orbital electrons of Ru ions on the square lattice. The d_{yz}, d_{zx}, and d_{xy} correspond to the d_{yz}, d_{zx}, and d_{xy} orbitals, respectively. (b) The band structure and (c) Fermi surface of our model for nondriven Sr_2RuO_4 at $T_b = 0.02$ eV for a $N_x \times N_y$ mesh with $N_x = N_y = 100$. In panel (b), the energies are measured from the chemical potential μ.

where $b_{ip}^\dagger$ and b_{ip} are the creation and annihilation operators, respectively, of a bath's fermion for mode p at site i, ϵ_p is the energy of a bath's fermion, and μ_b is its chemical potential. μ_b is determined in order that there is no current between the system and bath. This heat bath is supposed to be in equilibrium at temperature T_b.

3.3 *System-bath coupling Hamiltonian H_{sb}*

H_{sb} describes the coupling between the system and bath:[8,11,38]

$$H_{sb} = \sum_i \sum_p \sum_{a=d_{yz},d_{zx},d_{xy}} \sum_{\sigma=\uparrow,\downarrow} V_{pa\sigma}(c_{ia\sigma}^\dagger b_{ip} + b_{ip}^\dagger c_{ia\sigma}), \quad (35)$$

where $V_{pa\sigma}$ is the coupling constant. In this study, we treat the effects of H_{sb} as second-order perturbation. As a result, its main effect can be reduced to the damping.[8,11,38] Because of this damping, a nonequilibrium steady state could be achieved.[8,11,38]

4. Floquet Linear-response Theory

In this section, we formulate the time-averaged spin and charge off-diagonal dc conductivities in the nonequilibrium steady states of our periodically driven systems by using the Floquet linear-response theory.[8,11,27,30,38,49] In this theory, we set $\mathbf{A}(t) = \mathbf{A}_{pump}(t) + \mathbf{A}_{prob}(t)$ and treat the effects of $\mathbf{A}_{pump}(t)$ in the Floquet theory[1,2] and those of $\mathbf{A}_{prob}(t)$ in the linear-response theory.[21] Therefore, this is a theory for the pump-probe measurements[50] in which the spin or charge current is generated perpendicular to the probe field with the pump field (Fig. 1). In addition, this theory is a natural extension of the Kubo formula[21] for nondriven systems to the periodically driven systems.

4.1 *Time-averaged spin and charge off-diagonal dc conductivities σ_{yx}^S and σ_{yx}^C*

Since the effects of $\mathbf{A}_{prob}(t)$ are treated in the linear-response theory,[21] the spin and charge off-diagonal dc conductivities as functions of time, $\sigma_{yx}^S(t,t')$ and $\sigma_{yx}^C(t,t')$, are given by[11]

$$\sigma_{yx}^S(t,t') = \frac{1}{i\omega}\frac{\delta\langle j_S^y(t)\rangle}{\delta A_{prob}^x(t')}, \quad (36)$$

$$\sigma_{yx}^C(t,t') = \frac{1}{i\omega}\frac{\delta\langle j_C^y(t)\rangle}{\delta A_{prob}^x(t')}, \quad (37)$$

where $\langle j_S^y(t)\rangle$ and $\langle j_C^y(t)\rangle$ are the expectation values of the operators of the spin current and charge current densities, respectively. These expectation values should be taken over the states with both the pump and probe fields. Then, the operators of the spin and charge currents are given by[11]

$$J_S^y(t) = \sum_{\mathbf{k}} \sum_{a,b} \sum_\sigma v_{ab\sigma}^{(S)y}(\mathbf{k},t) c_{\mathbf{k}a\sigma}^\dagger(t) c_{\mathbf{k}b\sigma}(t), \quad (38)$$

$$J_C^y(t) = \sum_{\mathbf{k}} \sum_{a,b} \sum_\sigma v_{ab\sigma}^{(C)y}(\mathbf{k},t) c_{\mathbf{k}a\sigma}^\dagger(t) c_{\mathbf{k}b\sigma}(t), \quad (39)$$

where

$$v_{ab\sigma}^{(S)\nu}(\mathbf{k},t) = \frac{1}{2}\mathrm{sgn}(\sigma)\frac{\partial\epsilon_{ab}(\mathbf{k},t)}{\partial k_\nu}, \quad (40)$$

$$v_{ab\sigma}^{(C)\nu}(\mathbf{k},t) = (-e)\frac{\partial\epsilon_{ab}(\mathbf{k},t)}{\partial k_\nu}, \quad (41)$$

and $\mathrm{sgn}(\sigma) = 1$ or -1 for $\sigma = \uparrow$ or $\downarrow$, respectively. Note that Eqs. (38) and (39) can be derived by using the continuity equations.[11] We also note that $J_S^y(t) = Nj_S^y(t)$ and $J_C^y(t) = Nj_C^y(t)$ in our model due to $V = Na_{NN}^2 = N$, where V is the volume of the system.

$\sigma^{\rm S}_{yx}(t,t')$ and $\sigma^{\rm C}_{yx}(t,t')$ can be expressed in terms of nonequilibrium Green's functions.[11,49] Substituting Eqs. (38) and (39) into Eqs. (36) and (37), respectively, we have

$$\sigma^{\rm S}_{yx}(t,t') = \sigma^{\rm S(1)}_{yx}(t,t') + \sigma^{\rm S(2)}_{yx}(t,t'), \tag{42}$$

$$\sigma^{\rm C}_{yx}(t,t') = \sigma^{\rm C(1)}_{yx}(t,t') + \sigma^{\rm C(2)}_{yx}(t,t'), \tag{43}$$

where $\sigma^{\rm Q(1)}_{yx}(t,t')$ and $\sigma^{\rm Q(2)}_{yx}(t,t')$ (Q = S or C) are given by

$$\sigma^{\rm Q(1)}_{yx}(t,t') = \frac{-1}{\omega N}\sum_{\mathbf{k}}\sum_{a,b}\sum_{\sigma}\frac{\delta v^{({\rm Q})y}_{ab\sigma}(\mathbf{k},t)}{\delta A^{x}_{\rm prob}(t')}G^{<}_{b\sigma a\sigma}(\mathbf{k};t,t), \tag{44}$$

$$\sigma^{\rm Q(2)}_{yx}(t,t') = \frac{-1}{\omega N}\sum_{\mathbf{k}}\sum_{a,b}\sum_{\sigma}v^{({\rm Q})y}_{ab\sigma}(\mathbf{k},t)\frac{\delta G^{<}_{b\sigma a\sigma}(\mathbf{k};t,t)}{\delta A^{x}_{\rm prob}(t')}, \tag{45}$$

and $G^{<}_{b\sigma' a\sigma}(\mathbf{k};t,t')$ is the lesser Green's function,[11,51–53]

$$G^{<}_{b\sigma' a\sigma}(\mathbf{k};t,t') = i\langle c^{\dagger}_{\mathbf{k}a\sigma}(t')c_{\mathbf{k}b\sigma'}(t)\rangle. \tag{46}$$

We emphasize that the group velocities and Green's function appearing in the right-hand sides of Eqs. (44) and (45) are those with only the pump field (i.e., no probe field). This is an advantage of the linear-response theory.[21] In periodically driven cases, these quantities and the transport coefficients are of nonequilibrium. Meanwhile, in nondriven cases, these quantities are of equilibrium, although the transport coefficients are of nonequilibrium; this is sometimes misunderstood as if the transport coefficients were also of equilibrium. To rewrite Eq. (45), we use the equation,

$$\begin{aligned}\frac{\delta G^{<}_{b\sigma a\sigma}(\mathbf{k};t,t)}{\delta A^{x}_{\rm prob}(t')} &= -\sum_{c,d}\sum_{\sigma'}v^{({\rm C})x}_{cd\sigma'}(\mathbf{k},t')[G^{\rm R}_{b\sigma c\sigma'}(\mathbf{k};t,t')G^{<}_{d\sigma' a\sigma}(\mathbf{k};t',t)\\ &\quad + G^{<}_{b\sigma c\sigma'}(\mathbf{k};t,t')G^{\rm A}_{d\sigma' a\sigma}(\mathbf{k};t',t)],\end{aligned} \tag{47}$$

where $G^{\rm R}_{a\sigma b\sigma'}(\mathbf{k};t,t')$ and $G^{\rm A}_{a\sigma b\sigma'}(\mathbf{k};t,t')$ are the retarded and advanced Green's functions,[11,51–53]

$$G^{\rm R}_{a\sigma b\sigma'}(\mathbf{k};t,t') = -i\theta(t-t')\langle\{c_{\mathbf{k}a\sigma}(t),c^{\dagger}_{\mathbf{k}b\sigma'}(t')\}\rangle, \tag{48}$$

$$G^{\rm A}_{a\sigma b\sigma'}(\mathbf{k};t,t') = i\theta(t'-t)\langle\{c_{\mathbf{k}a\sigma}(t),c^{\dagger}_{\mathbf{k}b\sigma'}(t')\}\rangle. \tag{49}$$

Note that Eq. (47) is obtained by using the Dyson equation of the Green's functions and the Langreth rule.[8,54,55] Substituting Eq. (47) into Eq. (45), we get

$$\begin{aligned}\sigma^{\rm Q(2)}_{yx}(t,t') = \frac{1}{\omega N}\sum_{\mathbf{k}}\sum_{a,b,c,d}\sum_{\sigma,\sigma'}&v^{({\rm Q})y}_{ab\sigma}(\mathbf{k},t)v^{({\rm C})x}_{cd\sigma'}(\mathbf{k},t')\\ &\times[G^{\rm R}_{b\sigma c\sigma'}(\mathbf{k};t,t')G^{<}_{d\sigma' a\sigma}(\mathbf{k};t',t)\\ &+ G^{<}_{b\sigma c\sigma'}(\mathbf{k};t,t')G^{\rm A}_{d\sigma' a\sigma}(\mathbf{k};t',t)].\end{aligned} \tag{50}$$

The spin transport and charge transport in a nonequilibrium steady state of our periodically driven system can be described by the time-averaged spin and charge off-diagonal dc conductivities $\sigma^{\rm S}_{yx}$ and $\sigma^{\rm C}_{yx}$, respectively [see Figs. 4(d) and 4(a)]. $\sigma^{\rm Q}_{yx}$ (Q = S or C) is defined as

$$\sigma^{\rm Q}_{yx} = \lim_{\omega\to 0}\sigma^{\rm Q}_{yx}(\omega), \tag{51}$$

where

$$\sigma^{\rm Q}_{yx}(\omega) = {\rm Re}\int_0^{T_{\rm p}}\frac{dt_{\rm av}}{T_{\rm p}}\int_{-\infty}^{\infty}dt_{\rm rel}\,e^{i\omega t_{\rm rel}}\sigma^{\rm Q}_{yx}(t,t'), \tag{52}$$

$t_{\rm rel} = t - t'$, and $t_{\rm av} = (t+t')/2$. Note that the dc limit $\omega \to 0$ can be appropriately taken in the same way as for nondriven systems because the probe frequency ω is coupled to $t_{\rm rel}$ in the Fourier transformation, whereas the time average is taken with respect to $t_{\rm av}$. In Eq. (52), we have considered only the real part because we focus on the time-averaged dc conductivities in this paper. To calculate $\sigma^{\rm Q}_{yx}(\omega)$, we use the Floquet representation of the Green's functions.[11,56] In general, the Green's functions in a periodically driven system depend not only on $t_{\rm rel}$, but also on $t_{\rm av}$. Because of this property, we should perform two transformations to convert the Green's functions into the frequency functions:

$$G^{r}_{a\sigma b\sigma';n}(\mathbf{k};\omega) = \int_{-\infty}^{\infty}dt_{\rm rel}\,e^{i\omega t_{\rm rel}}\int_0^{T_{\rm p}}\frac{dt_{\rm av}}{T_{\rm p}}e^{in\Omega t_{\rm av}}G^{r}_{a\sigma b\sigma'}\left(\mathbf{k};t_{\rm av}+\frac{t_{\rm rel}}{2},t_{\rm av}-\frac{t_{\rm rel}}{2}\right), \tag{53}$$

where $G^{r}_{a\sigma b\sigma';n}(\mathbf{k};\omega)$'s ($r = {\rm R}, {\rm A}, <$) are defined in the range of $-\infty < \omega < \infty$. Since our Hamiltonian has the discrete time translation symmetry, we can restrict the range of frequency to $-\frac{\Omega}{2} \le \omega < \frac{\Omega}{2}$. This property can be taken into account by performing another transformation:

$$[G^{r}_{a\sigma b\sigma'}(\mathbf{k},\omega)]_{mn} = G^{r}_{a\sigma b\sigma';m-n}\left(\mathbf{k};\omega+\frac{m+n}{2}\Omega\right), \tag{54}$$

where $[G^{r}_{a\sigma b\sigma'}(\mathbf{k},\omega)]_{mn}$'s ($-\frac{\Omega}{2} \le \omega < \frac{\Omega}{2}$) are the Green's functions in the Floquet representation.[11,56] By combining Eqs. (52), (42)–(44), and (50) and using the Floquet representation of the Green's functions, we obtain

$$\begin{aligned}\sigma^{\rm Q}_{yx}(\omega) = \frac{1}{N}\sum_{\mathbf{k}}\sum_{a,b,c,d}\sum_{\sigma,\sigma'}&\int_{-\Omega/2}^{\Omega/2}\frac{d\omega'}{2\pi}\\ &\times\left\{{\rm tr}\left[v^{({\rm Q})y}_{ab\sigma}(\mathbf{k})\frac{G^{\rm R}_{b\sigma c\sigma'}(\mathbf{k},\omega'+\omega)-G^{\rm R}_{b\sigma c\sigma'}(\mathbf{k},\omega'-\omega)}{2\omega}v^{({\rm C})x}_{cd\sigma'}(\mathbf{k})G^{<}_{d\sigma' a\sigma}(\mathbf{k},\omega')\right]\right.\\ &\left.-{\rm tr}\left[v^{({\rm Q})y}_{ab\sigma}(\mathbf{k})G^{<}_{b\sigma c\sigma'}(\mathbf{k},\omega')v^{({\rm C})x}_{cd\sigma'}(\mathbf{k})\frac{G^{\rm A}_{d\sigma' a\sigma}(\mathbf{k},\omega'+\omega)-G^{\rm A}_{d\sigma' a\sigma}(\mathbf{k},\omega'-\omega)}{2\omega}\right]\right\},\end{aligned} \tag{55}$$

where ${\rm tr}(ABCD) = \sum_{m,l,n,q=-\infty}^{\infty}[A]_{ml}[B]_{ln}[C]_{nq}[D]_{qm}$, and m, l, n, and q are indices in the Floquet representation. For the derivation of Eq. (55), see Appendix A. Note that $[v^{({\rm Q})\nu}_{ab\sigma}(\mathbf{k})]_{mn}$ ($\nu = x, y$) is given by

$$[v^{({\rm Q})\nu}_{ab\sigma}(\mathbf{k})]_{mn} = \int_0^{T_{\rm p}}\frac{dt}{T_{\rm p}}e^{i(m-n)\Omega t}v^{({\rm Q})\nu}_{ab\sigma}(\mathbf{k},t), \tag{56}$$

where $v^{(\mathrm{S})\nu}_{ab\sigma}(\mathbf{k},t)$ and $v^{(\mathrm{C})\nu}_{ab\sigma}(\mathbf{k},t)$ have been defined in Eqs. (40) and (41), respectively. Combining Eq. (55) with Eq. (51), we get

$$\sigma^{\mathrm{S}}_{yx} = \frac{1}{N}\sum_{\mathbf{k}}\sum_{a,b,c,d}\sum_{\sigma,\sigma'}\int_{-\Omega/2}^{\Omega/2}\frac{d\omega'}{2\pi}\left\{\mathrm{tr}\left[v^{(\mathrm{S})y}_{ab\sigma}(\mathbf{k})\frac{\partial G^{\mathrm{R}}_{b\sigma c\sigma'}(\mathbf{k},\omega')}{\partial\omega'}v^{(\mathrm{C})x}_{cd\sigma'}(\mathbf{k})G^{<}_{d\sigma' a\sigma}(\mathbf{k},\omega')\right]\right.$$
$$\left. - \mathrm{tr}\left[v^{(\mathrm{S})y}_{ab\sigma}(\mathbf{k})G^{<}_{b\sigma c\sigma'}(\mathbf{k},\omega')v^{(\mathrm{C})x}_{cd\sigma'}(\mathbf{k})\frac{\partial G^{\mathrm{A}}_{d\sigma' a\sigma}(\mathbf{k},\omega')}{\partial\omega'}\right]\right\}, \tag{57}$$

and

$$\sigma^{\mathrm{C}}_{yx} = \frac{1}{N}\sum_{\mathbf{k}}\sum_{a,b,c,d}\sum_{\sigma,\sigma'}\int_{-\Omega/2}^{\Omega/2}\frac{d\omega'}{2\pi}\left\{\mathrm{tr}\left[v^{(\mathrm{C})y}_{ab\sigma}(\mathbf{k})\frac{\partial G^{\mathrm{R}}_{b\sigma c\sigma'}(\mathbf{k},\omega')}{\partial\omega'}v^{(\mathrm{C})x}_{cd\sigma'}(\mathbf{k})G^{<}_{d\sigma' a\sigma}(\mathbf{k},\omega')\right]\right.$$
$$\left. - \mathrm{tr}\left[v^{(\mathrm{C})y}_{ab\sigma}(\mathbf{k})G^{<}_{b\sigma c\sigma'}(\mathbf{k},\omega')v^{(\mathrm{C})x}_{cd\sigma'}(\mathbf{k})\frac{\partial G^{\mathrm{A}}_{d\sigma' a\sigma}(\mathbf{k},\omega')}{\partial\omega'}\right]\right\}. \tag{58}$$

The Green's functions appearing in Eqs. (57) and (58) can be determined in the following way. For our periodically driven system, the Green's functions are determined from the Dyson equation in the matrix form,[11,52,57]

$$G = G_0 + G_0\Sigma G, \tag{59}$$

where G is the matrix of the Green's functions with H_{sb},

$$G = \begin{pmatrix} G^{\mathrm{R}} & G^{\mathrm{K}} \\ 0 & G^{\mathrm{A}} \end{pmatrix}, \tag{60}$$

G_0 is the matrix of the Green's functions without H_{sb},

$$G_0 = \begin{pmatrix} G^{\mathrm{R}}_0 & G^{\mathrm{K}}_0 \\ 0 & G^{\mathrm{A}}_0 \end{pmatrix}, \tag{61}$$

and Σ is the matrix of the self-energies due to the second-order perturbation with respect to H_{sb},

$$\Sigma = \begin{pmatrix} \Sigma^{\mathrm{R}} & \Sigma^{\mathrm{K}} \\ 0 & \Sigma^{\mathrm{A}} \end{pmatrix}. \tag{62}$$

In Eqs. (60)–(62), the superscripts R, A, and K represent the retarded, advanced, and Keldysh components, respectively. These three components are related to the lesser component as follows:

$$G^{<} = \frac{1}{2}(G^{\mathrm{K}} - G^{\mathrm{R}} + G^{\mathrm{A}}). \tag{63}$$

The retarded, advanced, and Keldysh components of the self-energies can be obtained by using the second-order perturbation theory; the results are

$$[\Sigma^{\mathrm{R}}_{a\sigma b\sigma'}(\mathbf{k},\omega)]_{mn} = -i\delta_{m,n}\delta_{a,b}\delta_{\sigma,\sigma'}\Gamma, \tag{64}$$

$$[\Sigma^{\mathrm{A}}_{a\sigma b\sigma'}(\mathbf{k},\omega)]_{mn} = +i\delta_{m,n}\delta_{a,b}\delta_{\sigma,\sigma'}\Gamma, \tag{65}$$

$$[\Sigma^{\mathrm{K}}_{a\sigma b\sigma'}(\mathbf{k},\omega)]_{mn} = -2i\delta_{m,n}\delta_{a,b}\delta_{\sigma,\sigma'}\Gamma\tanh\frac{\omega+m\Omega}{2T_{\mathrm{b}}}, \tag{66}$$

where Γ is the damping. In deriving these equations, we have omitted the real parts and replaced $\pi\sum_p V_{pa\sigma}V_{pb\sigma'}\delta(\omega + m\Omega - \epsilon_p + \mu_{\mathrm{b}})$ by $\Gamma\delta_{a,b}\delta_{\sigma,\sigma'}$ for simplicity.[11] Such simplification may be sufficient because the main effect of H_{sb} is to induce the damping, which makes the system the nonequilibrium steady state.[8,11,38] Then, Eq. (59) can be rewritten as

$$G^{-1} = G_0^{-1} - \Sigma, \tag{67}$$

where

$$G^{-1} = \begin{pmatrix} (G^{-1})^{\mathrm{R}} & (G^{-1})^{\mathrm{K}} \\ 0 & (G^{-1})^{\mathrm{A}} \end{pmatrix}, \tag{68}$$

$$G_0^{-1} = \begin{pmatrix} (G_0^{-1})^{\mathrm{R}} & (G_0^{-1})^{\mathrm{K}} \\ 0 & (G_0^{-1})^{\mathrm{A}} \end{pmatrix}. \tag{69}$$

For our model, the retarded, advanced, and Keldysh components of the matrix G^{-1} are given by

$$[(G^{-1})^{\mathrm{R}}_{a\sigma b\sigma'}(\mathbf{k},\omega)]_{mn} = (\omega+\mu+m\Omega+i\Gamma)\delta_{m,n}\delta_{a,b}\delta_{\sigma,\sigma'} - \xi^{\sigma\sigma'}_{ab}\delta_{m,n} - [\epsilon_{ab}(\mathbf{k})]_{mn}\delta_{\sigma,\sigma'}, \tag{70}$$

$$[(G^{-1})^{\mathrm{A}}_{a\sigma b\sigma'}(\mathbf{k},\omega)]_{mn} = (\omega+\mu+m\Omega-i\Gamma)\delta_{m,n}\delta_{a,b}\delta_{\sigma,\sigma'} - \xi^{\sigma\sigma'}_{ab}\delta_{m,n} - [\epsilon_{ab}(\mathbf{k})]_{mn}\delta_{\sigma,\sigma'}, \tag{71}$$

$$[(G^{-1})^{\mathrm{K}}_{a\sigma b\sigma'}(\mathbf{k},\omega)]_{mn} = 2i\delta_{m,n}\delta_{a,b}\delta_{\sigma,\sigma'}\Gamma\tanh\frac{\omega+m\Omega}{2T_{\mathrm{b}}}, \tag{72}$$

where

$$[\epsilon_{ab}(\mathbf{k})]_{mn} = \int_0^{T_{\mathrm{p}}}\frac{dt}{T_{\mathrm{p}}}e^{i(m-n)\Omega t}\epsilon_{ab}(\mathbf{k},t). \tag{73}$$

For $[\epsilon_{ab}(\mathbf{k})]_{mn}$ of Sr_2RuO_4 driven by BCPL, see Appendix B; for that of Sr_2RuO_4 driven by CPL or LPL, see Ref. 11. In deriving Eq. (72), we have chosen the Keldysh component of the matrix G_0^{-1} to be zero because it contains the information about the initial condition. This treatment may be valid to describe a nonequilibrium steady state with finite damping[7,8,11,38] because a nonequilibrium steady state should be independent of a choice of the initial condition. Note that the retarded and advanced components of the matrix G_0^{-1} are obtained by replacing Γ in Eqs. (70) and (71), respectively, by a positive infinitesimal. Because of the matrix relation $G^{-1}G = 1$, the components of the inverse matrices satisfy

$$(G^{\mathrm{R}})^{-1} = (G^{-1})^{\mathrm{R}}, \tag{74}$$

$$(G^{\mathrm{A}})^{-1} = (G^{-1})^{\mathrm{A}}, \tag{75}$$

$$G^{\mathrm{K}} = -G^{\mathrm{R}}(G^{-1})^{\mathrm{K}}G^{\mathrm{A}}. \tag{76}$$

Therefore, we can obtain the retarded and advanced Green's functions with H_{sb} by using Eqs. (70) and (74) and Eqs. (71) and (75), respectively. We can also calculate the Keldysh Green's function with H_{sb} by combining Eq. (76) with Eq. (72) and the obtained retarded and advanced Green's functions. Using Eq. (63) and the obtained three Green's

functions, we finally obtain the lesser Green's function with $H_{\rm sb}$.

4.2 *The other off-diagonal dc conductivities $\tilde{\sigma}^S_{xy}$, σ^C_{xy}, $\bar{\tilde{\sigma}}^S_{xy}$, and $\bar{\sigma}^C_{xy}$*

To discuss the Onsager reciprocal relations, we need to consider $\tilde{\sigma}^{\rm S}_{xy}$ and $\sigma^{\rm C}_{xy}$. Here $\tilde{\sigma}^{\rm S}_{xy}$ or $\sigma^{\rm C}_{xy}$ is the time-averaged off-diagonal dc conductivity for the charge current along the x axis perpendicular to the probe spin field or electric field, respectively, applied along the y axis with the pump field $\mathbf{A}_{\rm pump}(t)$ [see Figs. 4(f) and 4(c)]. These conductivities are given by

$$\tilde{\sigma}^{\rm S}_{xy} = \frac{1}{N}\sum_{\mathbf{k}}\sum_{a,b,c,d}\sum_{\sigma,\sigma'}\int_{-\Omega/2}^{\Omega/2}\frac{d\omega'}{2\pi}\left\{\mathrm{tr}\left[v^{({\rm C})x}_{ab\sigma}(\mathbf{k})\frac{\partial G^{\rm R}_{b\sigma c\sigma'}(\mathbf{k},\omega')}{\partial\omega'}v^{({\rm S})y}_{cd\sigma'}(\mathbf{k})G^{<}_{d\sigma' a\sigma}(\mathbf{k},\omega')\right]\right.$$
$$\left.-\mathrm{tr}\left[v^{({\rm C})x}_{ab\sigma}(\mathbf{k})G^{<}_{b\sigma c\sigma'}(\mathbf{k},\omega')v^{({\rm S})y}_{cd\sigma'}(\mathbf{k})\frac{\partial G^{\rm A}_{d\sigma' a\sigma}(\mathbf{k},\omega')}{\partial\omega'}\right]\right\}, \tag{77}$$

and

$$\sigma^{\rm C}_{xy} = \frac{1}{N}\sum_{\mathbf{k}}\sum_{a,b,c,d}\sum_{\sigma,\sigma'}\int_{-\Omega/2}^{\Omega/2}\frac{d\omega'}{2\pi}\left\{\mathrm{tr}\left[v^{({\rm C})x}_{ab\sigma}(\mathbf{k})\frac{\partial G^{\rm R}_{b\sigma c\sigma'}(\mathbf{k},\omega')}{\partial\omega'}v^{({\rm C})y}_{cd\sigma'}(\mathbf{k})G^{<}_{d\sigma' a\sigma}(\mathbf{k},\omega')\right]\right.$$
$$\left.-\mathrm{tr}\left[v^{({\rm C})x}_{ab\sigma}(\mathbf{k})G^{<}_{b\sigma c\sigma'}(\mathbf{k},\omega')v^{({\rm C})y}_{cd\sigma'}(\mathbf{k})\frac{\partial G^{\rm A}_{d\sigma' a\sigma}(\mathbf{k},\omega')}{\partial\omega'}\right]\right\}. \tag{78}$$

Here Eq. (77) has been obtained by replacing $v^{({\rm S})y}_{ab\sigma}(\mathbf{k})$'s and $v^{({\rm C})x}_{cd\sigma'}(\mathbf{k})$'s in Eq. (57) by $v^{({\rm C})x}_{ab\sigma}(\mathbf{k})$'s and $v^{({\rm S})y}_{cd\sigma'}(\mathbf{k})$'s, respectively; and Eq. (78) has been obtained by replacing $v^{({\rm C})y}_{ab\sigma}(\mathbf{k})$'s and $v^{({\rm C})x}_{cd\sigma'}(\mathbf{k})$'s in Eq. (58) by $v^{({\rm C})x}_{ab\sigma}(\mathbf{k})$'s and $v^{({\rm C})y}_{cd\sigma'}(\mathbf{k})$'s, respectively. The quantities appearing in Eqs. (77) and (78) can be determined in the same way as those appearing in Eqs. (57) and (58).

In addition, we need to consider $\bar{\tilde{\sigma}}^{\rm S}_{xy}$ and $\bar{\sigma}^{\rm C}_{xy}$. Here $\bar{\tilde{\sigma}}^{\rm S}_{xy}$ or $\bar{\sigma}^{\rm C}_{xy}$ is the time-averaged off-diagonal dc conductivity for the charge current along the x axis perpendicular to the probe spin field or electric field, respectively, applied along the y axis with the pump field $\mathbf{A}_{\rm pump}(-t)$ [see Figs. 4(e) and 4(b)]. These conductivities are given by

$$\bar{\tilde{\sigma}}^{\rm S}_{xy} = \frac{1}{N}\sum_{\mathbf{k}}\sum_{a,b,c,d}\sum_{\sigma,\sigma'}\int_{-\Omega/2}^{\Omega/2}\frac{d\omega'}{2\pi}\left\{\mathrm{tr}\left[\bar{v}^{({\rm C})x}_{ab\sigma}(\mathbf{k})\frac{\partial \bar{G}^{\rm R}_{b\sigma c\sigma'}(\mathbf{k},\omega')}{\partial\omega'}\bar{v}^{({\rm S})y}_{cd\sigma'}(\mathbf{k})\bar{G}^{<}_{d\sigma' a\sigma}(\mathbf{k},\omega')\right]\right.$$
$$\left.-\mathrm{tr}\left[\bar{v}^{({\rm C})x}_{ab\sigma}(\mathbf{k})\bar{G}^{<}_{b\sigma c\sigma'}(\mathbf{k},\omega')\bar{v}^{({\rm S})y}_{cd\sigma'}(\mathbf{k})\frac{\partial \bar{G}^{\rm A}_{d\sigma' a\sigma}(\mathbf{k},\omega')}{\partial\omega'}\right]\right\}, \tag{79}$$

and

$$\bar{\sigma}^{\rm C}_{xy} = \frac{1}{N}\sum_{\mathbf{k}}\sum_{a,b,c,d}\sum_{\sigma,\sigma'}\int_{-\Omega/2}^{\Omega/2}\frac{d\omega'}{2\pi}\left\{\mathrm{tr}\left[\bar{v}^{({\rm C})x}_{ab\sigma}(\mathbf{k})\frac{\partial \bar{G}^{\rm R}_{b\sigma c\sigma'}(\mathbf{k},\omega')}{\partial\omega'}\bar{v}^{({\rm C})y}_{cd\sigma'}(\mathbf{k})\bar{G}^{<}_{d\sigma' a\sigma}(\mathbf{k},\omega')\right]\right.$$
$$\left.-\mathrm{tr}\left[\bar{v}^{({\rm C})x}_{ab\sigma}(\mathbf{k})\bar{G}^{<}_{b\sigma c\sigma'}(\mathbf{k},\omega')\bar{v}^{({\rm C})y}_{cd\sigma'}(\mathbf{k})\frac{\partial \bar{G}^{\rm A}_{d\sigma' a\sigma}(\mathbf{k},\omega')}{\partial\omega'}\right]\right\}. \tag{80}$$

Here $[\bar{v}^{({\rm Q})\nu}_{ab\sigma}(\mathbf{k})]_{mn}$ $(\nu = x, y)$ is given by

$$[\bar{v}^{({\rm Q})\nu}_{ab\sigma}(\mathbf{k})]_{mn} = \int_0^{T_{\rm p}}\frac{dt}{T_{\rm p}}e^{i(m-n)\Omega t}v^{({\rm Q})\nu}_{ab\sigma}(\mathbf{k},-t), \tag{81}$$

and $[\bar{G}^r_{a\sigma b\sigma'}(\mathbf{k},\omega)]_{mn}$'s are determined by replacing Eqs. (70)–(76) by

$$[(\bar{G}^{-1})^{\rm R}_{a\sigma b\sigma'}(\mathbf{k},\omega)]_{mn} = (\omega+\mu+m\Omega+i\Gamma)\delta_{m,n}\delta_{a,b}\delta_{\sigma,\sigma'} - \xi^{\sigma\sigma'}_{ab}\delta_{m,n} - [\bar{\epsilon}_{ab}(\mathbf{k})]_{mn}\delta_{\sigma,\sigma'}, \tag{82}$$

$$[(\bar{G}^{-1})^{\rm A}_{a\sigma b\sigma'}(\mathbf{k},\omega)]_{mn} = (\omega+\mu+m\Omega-i\Gamma)\delta_{m,n}\delta_{a,b}\delta_{\sigma,\sigma'} - \xi^{\sigma\sigma'}_{ab}\delta_{m,n} - [\bar{\epsilon}_{ab}(\mathbf{k})]_{mn}\delta_{\sigma,\sigma'}, \tag{83}$$

$$[(\bar{G}^{-1})^{\rm K}_{a\sigma b\sigma'}(\mathbf{k},\omega)]_{mn} = 2i\delta_{m,n}\delta_{a,b}\delta_{\sigma,\sigma'}\Gamma\tanh\frac{\omega+m\Omega}{2T_{\rm b}}, \tag{84}$$

$$[\bar{\epsilon}_{ab}(\mathbf{k})]_{mn} = \int_0^{T_{\rm p}}\frac{dt}{T_{\rm p}}e^{i(m-n)\Omega t}\epsilon_{ab}(\mathbf{k},-t), \tag{85}$$

$$(\bar{G}^{\rm R})^{-1} = (\bar{G}^{-1})^{\rm R}, \tag{86}$$

$$(\bar{G}^{\rm A})^{-1} = (\bar{G}^{-1})^{\rm A}, \tag{87}$$

$$\bar{G}^{\rm K} = -\bar{G}^{\rm R}(\bar{G}^{-1})^{\rm K}\bar{G}^{\rm A}, \tag{88}$$

and performing the similar procedures to those used to determine $[G^r_{a\sigma b\sigma'}(\mathbf{k},\omega)]_{mn}$'s. Namely, the group velocities and Green's functions appearing in Eqs. (79) and (80) are calculated with $\mathbf{A}_{\rm pump}(-t)$ in the similar way to those with $\mathbf{A}_{\rm pump}(t)$. For $[\bar{\epsilon}_{ab}(\mathbf{k})]_{mn}$ of Sr_2RuO_4 driven by BCPL, see Appendix C.

4.3 *General remarks about the applicability*

First, the Floquet linear-response theory is applicable to the periodically driven systems under the application of the pump field. This is because the discrete time translational symmetry is utilized in the Floquet theory.

Then, our theory has wider applicability than the theories using a high-frequency expansion. This expansion has been often used to analyze many periodically driven sys-

tems.[3,8,30,58,59] It may be sufficient for a periodically driven electron system if the light frequency is much larger than the bandwidth of the system. Meanwhile, our theory does not have such a restriction because the Floquet theory used here is free from the constraint on the frequency.

The applicability of our theory is also wider than that of the theories in which the time-averaged off-diagonal dc conductivities are expressed in terms of the Berry curvature. In the limit $\Gamma \to 0$, these conductivities could be linked to the Berry curvature.[7,8] This is similar to the AHE and SHE in nondriven systems.[60–62] However, for finite Γ, the anomalous Hall or spin Hall conductivity in nondriven systems contains not only the Berry-curvature term, but also the others, including the so-called Fermi-surface term,[60–63] which is distinct from the Berry-curvature term. Furthermore, the Fermi-surface term dominates the intrinsic AHE and SHE at finite Γ.[46,60–62] The similar crossover can be realized for the Hall conductivity with the magnetic field: the Hall conductivity in the strong-field case $\omega_c\tau \gg 1$ can be approximated by the Berry-curvature term,[64] whereas that in the weak-field case $\omega_c\tau \ll 1$ is described by the Fermi-surface term.[65] Here ω_c represents the energy gap between Landau levels, and τ is inversely proportional to the damping. Namely, the Berry-curvature term is dominant if the band splitting which contributes to the Hall conductivity is much larger than the broadening in the single-particle spectrum; otherwise, the Fermi-surface term is dominant. Importantly, these terms are automatically included in the conductivities derived from the Kubo formula without any additional approximation. Moreover, the limit $\Gamma \to 0$ is unrealistic in periodically driven systems because the finite Γ is required to realize a nonequilibrium steady state with the heating due to the pump field. Therefore, we will study the time-averaged spin and charge off-diagonal dc conductivities without simplification using the Berry curvature.

5. Numerical Results

In this section, we show the time-averaged spin and charge off-diagonal dc conductivities calculated numerically for Sr_2RuO_4 driven by CPL, LPL, or BCPL at $\beta = 2$ or 3. In Sect. 5.1, we focus on the time-averaged spin off-diagonal dc conductivities. In all the cases considered, the Onsager reciprocal relations argued in Sect. 2.2.2 are satisfied and the main terms are given by the antisymmetric parts. In Sect. 5.2, we turn to the time-averaged charge off-diagonal dc conductivities. Although the Onsager reciprocal relations argued in Sect. 2.1.2 are satisfied, their main terms depend on the polarization of light. In the case with CPL or LPL, the main term is the antisymmetric or symmetric part, respectively. Then, in the cases with BCPL at $(\beta,\theta) = (2,\frac{\pi}{4})$, $(2,\frac{3\pi}{4})$, $(3,\frac{\pi}{4})$, $(3,\frac{\pi}{2})$, and $(3,\frac{3\pi}{4})$, the main term is the antisymmetric part in the range of $0 \le u \le 0.4$, whereas it is the symmetric part in the range of $0.5 \le u \le 1$. Here $u = eA_0$ is the dimensionless quantity. Meanwhile, in the cases with BCPL at $(\beta,\theta) = (2,0)$, $(2,\frac{\pi}{2})$, $(2,\pi)$, $(3,0)$, and $(3,\pi)$, σ^{C}_{yx} is almost vanishing in the range of $0.5 \le u \le 1$, although its main term is the antisymmetric part in the range of $0 \le u \le 0.4$. These results are consistent with our general arguments made in Sect. 2.

We numerically evaluated Eqs. (57), (58), and (77)–(80) using the following four procedures. First, we calculated the momentum summation by dividing the first Brillouin zone into a $N_x \times N_y$ mesh. Second, we performed the frequency integration using $\int_{-\Omega/2}^{\Omega/2} d\omega' F(\omega') \approx \sum_{s=0}^{W-1} \Delta\omega' F(\omega'_s)$, where $\omega'_s = -\Omega/2 + s\Delta\omega'$, and $\omega'_W = \Omega/2$. Third, we calculated the frequency derivatives of the Green's functions by using $\frac{\partial F(\omega')}{\partial\omega'} \approx \frac{F(\omega'+\Delta\omega')-F(\omega'-\Delta\omega')}{2\Delta\omega'}$. Fourth, we replaced the summations over the Floquet indices, $\sum_{m,l,n,q=-\infty}^{\infty}$, by $\sum_{m,l,n,q=-n_{\max}}^{n_{\max}}$.

In the actual calculations, we set $N_x = N_y = 100$, $\Delta\omega' = 0.005$ eV, $\Gamma = 0.01$ eV, $T_b = 0.02$ eV, and $\Omega = 6$ eV. This Ω is larger than the bandwidth of the nondriven system [Fig. 5(b)], which means that the light is off-resonant. We also set $n_{\max} = 1$ except the results for $n_{\max} = 0$. Note that the calculations with $n_{\max} = 0$ include the light-induced corrections due to only the zeroth-order Bessel functions, whereas the calculations with $n_{\max} = 1$ include those due to not only the zeroth- and first-order Bessel functions, but also the higher-order Bessel functions (see Appendix B). In Appendix D, we show that the results obtained for $n_{\max} = 1$ and 2 are qualitatively the same in the case with BCPL at $\beta = 2$, $\theta = \frac{\pi}{4}$, and $\Omega = 6$ eV. The similar property holds in the case with CPL.[11] Therefore, setting $n_{\max} = 1$ may be reasonable in periodically driven Sr_2RuO_4 at $\Omega = 6$ eV.

The reasons for presenting the numerical results are three fold. First, the consistency between our general arguments and numerical results supports the correctness of the results obtained in them. Second, the numerical results for a specific model may help to better understand the Onsager reciprocal relations in the periodically driven systems. Third, the numerical results can determine whether the time-averaged spin and charge off-diagonal dc conductivities are dominated by the symmetric or antisymmetric parts even in the cases with BCPL. In the cases with BCPL, the dominant terms cannot be determined from the general arguments due to the lack of a simple relation between the pump field and its time-reversal counterpart, as we have explained in Sects. 2.1.2 and 2.2.2.

5.1 *Time-averaged spin off-diagonal dc conductivities*

We compare the numerically calculated σ^{S}_{yx}, $\bar{\tilde{\sigma}}^{S}_{xy}$, and $\tilde{\sigma}^{S}_{xy}$ for Sr_2RuO_4 driven by CPL, LPL, or BCPL. The Onsager reciprocal relations are satisfied in all the cases considered. Furthermore, the main term of σ^{S}_{yx} is given by the antisymmetric part. Therefore, σ^{S}_{yx} can be regarded as the spin Hall conductivity in all the cases considered.

5.1.1 *Case with CPL or LPL*

Figure 6(a) shows the u dependences of σ^{S}_{yx}, $\bar{\tilde{\sigma}}^{S}_{xy}$, and $\tilde{\sigma}^{S}_{xy}$ for Sr_2RuO_4 driven by LCPL. These conductivities satisfy $\sigma^{S}_{yx} = -\bar{\tilde{\sigma}}^{S}_{xy}$ and $\sigma^{S}_{yx} = -\tilde{\sigma}^{S}_{xy}$, which correspond to Eqs. (19) and (23), respectively. The former means that σ^{S}_{yx} satisfies the Onsager reciprocal relation, whereas the latter means that it is antisymmetric. Namely, these results demonstrate the validity of Eqs. (19) and (23).

Then, Fig. 6(b) shows the u dependences of σ^{S}_{yx} and $\tilde{\sigma}^{S}_{xy}$ for Sr_2RuO_4 driven by LPL. Note that in the case of LPL, $\bar{\tilde{\sigma}}^{S}_{xy} = \tilde{\sigma}^{S}_{xy}$ holds. As well as the case with CPL, the Onsager reciprocal relation is satisfied with LPL, and σ^{S}_{yx} is given by the antisymmetric part. Therefore, Eq. (24) is also validated.

5.1.2 *Cases with BCPL*

Figure 7(a) shows the u dependences of σ^{S}_{yx} for Sr_2RuO_4

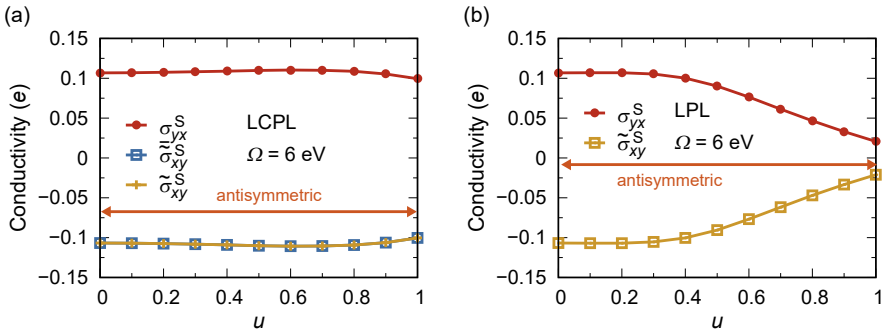

Fig. 6. (Color online) The u ($= eA_0$) dependences of $\sigma^{\rm S}_{yx}$, $\tilde{\bar{\sigma}}^{\rm S}_{xy}$, and $\tilde{\sigma}^{\rm S}_{xy}$ for Sr_2RuO_4 driven by (a) LCPL and (b) LPL at $\Omega = 6$ eV. The pump fields of LCPL and LPL have been defined in Eqs. (4) and (11), respectively. For $\sigma^{\rm S}_{yx}$, $\tilde{\bar{\sigma}}^{\rm S}_{xy}$, and $\tilde{\sigma}^{\rm S}_{xy}$, see Figs. 4(d), 4(e), and 4(f), respectively. In the case with LPL, $\tilde{\bar{\sigma}}^{\rm S}_{xy} = \tilde{\sigma}^{\rm S}_{xy}$.

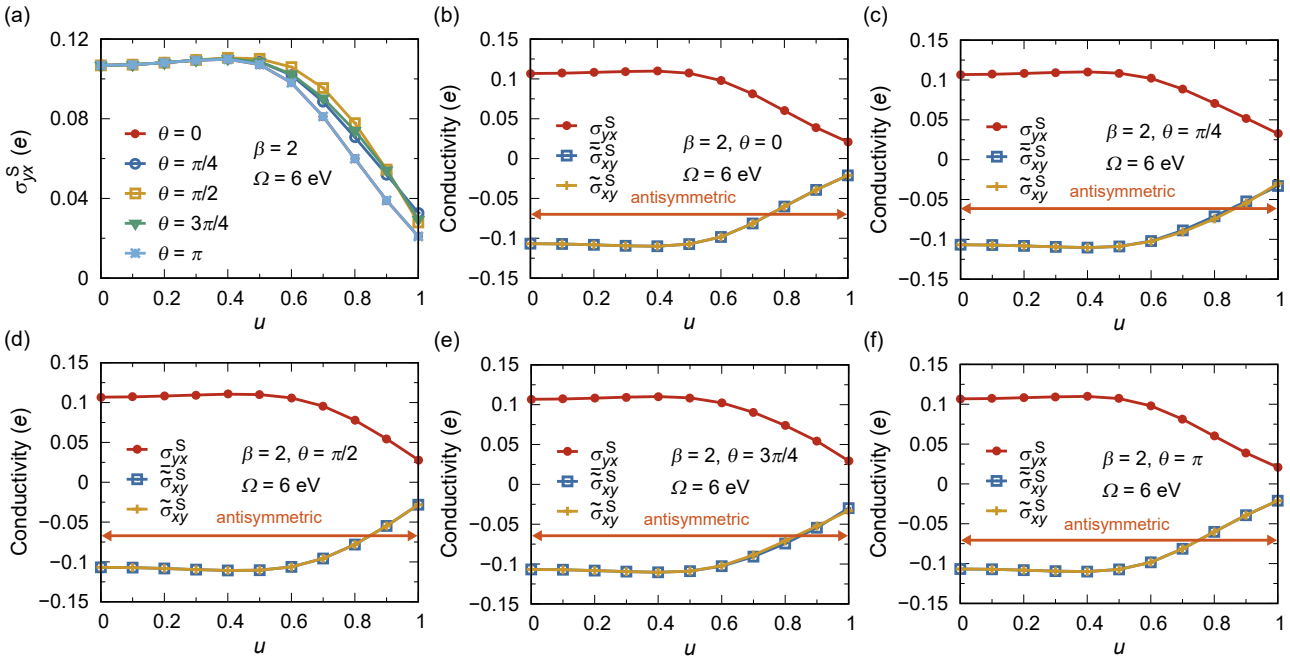

Fig. 7. (Color online) (a) The u ($= eA_0$) dependences of $\sigma^{\rm S}_{yx}$ for Sr_2RuO_4 driven by BCPL at $\beta = 2$ and $\Omega = 6$ eV with $\theta = 0$, $\frac{\pi}{4}$, $\frac{\pi}{2}$, $\frac{3\pi}{4}$, and π. The pump field of BCPL has been defined in Eqs. (12) and (13). For $\sigma^{\rm S}_{yx}$, see Fig. 4(d). The u dependences of $\sigma^{\rm S}_{yx}$, $\tilde{\bar{\sigma}}^{\rm S}_{xy}$, and $\tilde{\sigma}^{\rm S}_{xy}$ for Sr_2RuO_4 driven by BCPL at $\beta = 2$ and $\Omega = 6$ eV with (b) $\theta = 0$, (c) $\theta = \frac{\pi}{4}$, (d) $\theta = \frac{\pi}{2}$, (e) $\theta = \frac{3\pi}{4}$, and (f) $\theta = \pi$. For $\tilde{\bar{\sigma}}^{\rm S}_{xy}$, and $\tilde{\sigma}^{\rm S}_{xy}$, see Figs. 4(e) and 4(f), respectively.

driven by BCPL at $\beta = 2$ and $\theta = 0$, $\frac{\pi}{4}$, $\frac{\pi}{2}$, $\frac{3\pi}{4}$, and π. $\sigma^{\rm S}_{yx}$ is almost independent of θ in the range of $0 \le u \le 0.4$, whereas it depends on θ in the range of $0.5 \le u \le 1$. This θ dependence may arise from the light-induced corrections due to the higher-order Bessel functions for moderately large u, as we will discuss in Sect. 6.1. The nearly monotonically decreasing u dependences may be due to the dynamical localization, the reduction in the kinetic energy due to the zeroth-order Bessel function in the Peierls phase factor. Note that the dynamical localization can be described by the time-averaged Hamiltonian, in which the zeroth-order Bessel function leads to the correction to the hopping integrals. In fact, the almost monotonically decreasing u dependence can be reproduced by the $\sigma^{\rm S}_{yx}$ calculated numerically with $n_{\rm max} = 0$, in which only the zeroth-order Bessel function gives the light-induced corrections [Fig. 8(a)].

In addition, Figs. 7(b)–7(f) show the u dependences of $\sigma^{\rm S}_{yx}$, $\tilde{\bar{\sigma}}^{\rm S}_{xy}$, and $\tilde{\sigma}^{\rm S}_{xy}$ for Sr_2RuO_4 driven by BCPL at $\beta = 2$ and $\theta = 0$, $\frac{\pi}{4}$, $\frac{\pi}{2}$, $\frac{3\pi}{4}$, and π. As well as the cases with CPL and LPL, the Onsager reciprocal relation $\sigma^{\rm S}_{yx} = -\tilde{\bar{\sigma}}^{\rm S}_{xy}$ holds. Furthermore, the main term is the antisymmetric part. This may be surprising because the Onsager reciprocal relation in this case does not restrict $\sigma^{\rm S}_{yx}$ to the antisymmetric part [see Eq. (25)].

The similar results are obtained at $\beta = 3$. Figure 9(a) shows the u dependences of $\sigma^{\rm S}_{yx}$ in Sr_2RuO_4 driven by BCPL at $\beta = 3$ and $\theta = 0$, $\frac{\pi}{4}$, $\frac{\pi}{2}$, $\frac{3\pi}{4}$, and π. $\sigma^{\rm S}_{yx}$ is almost independent of θ in the range of $0 \le u \le 0.7$, whereas it depends on θ in the range of $0.8 \le u \le 1$. As we will discuss in Sect. 6.1, we can understand this θ dependence in a similar way to that obtained at $\beta = 2$. Then, Figs. 9(b)–9(f) show the relations among $\sigma^{\rm S}_{yx}$, $\tilde{\bar{\sigma}}^{\rm S}_{xy}$, and $\tilde{\sigma}^{\rm S}_{xy}$ as functions of u at $\beta = 3$ and $\theta = 0$, $\frac{\pi}{4}$, $\frac{\pi}{2}$, $\frac{3\pi}{4}$, and π. At these θ's, the Onsager reciprocal relation holds and the antisymmetric part gives the main contribution. Note that the almost monotonically decreasing u dependence is reproducible by the $n_{\rm max} = 0$ terms [Fig. 8(b)].

Before showing the results of the time-averaged charge off-diagonal dc conductivities, we comment on the role of the SOC. Figure 10(a) compares the u dependences of $\sigma^{\rm S}_{yx}$ for Sr_2RuO_4 driven by BCPL at $\beta = 2$ and $\theta = 0$ with and without the SOC. [Note that in our model, the SOC is the *LS*

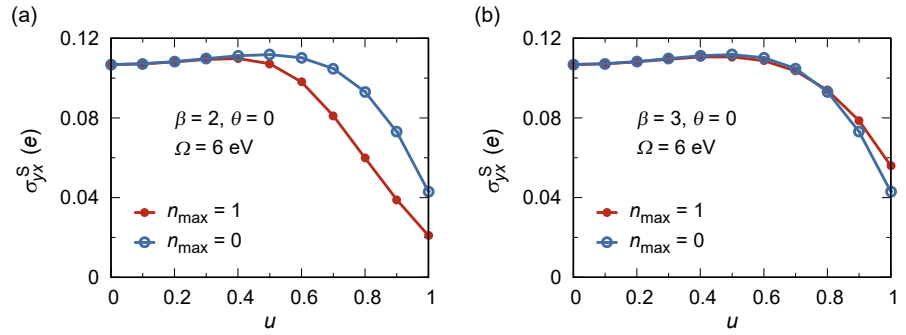

Fig. 8. (Color online) The u ($= eA_0$) dependences of σ^{S}_{yx} for Sr_2RuO_4 driven by BCPL at (a) $\beta = 2$ and (b) $\beta = 3$, $\theta = 0$, and $\Omega = 6$ eV with $n_{max} = 1$ and 0. Here n_{max} is the upper limit of the summation over the Floquet indices, i.e., $\sum_{m,l,n,q=-n_{max}}^{n_{max}}$.

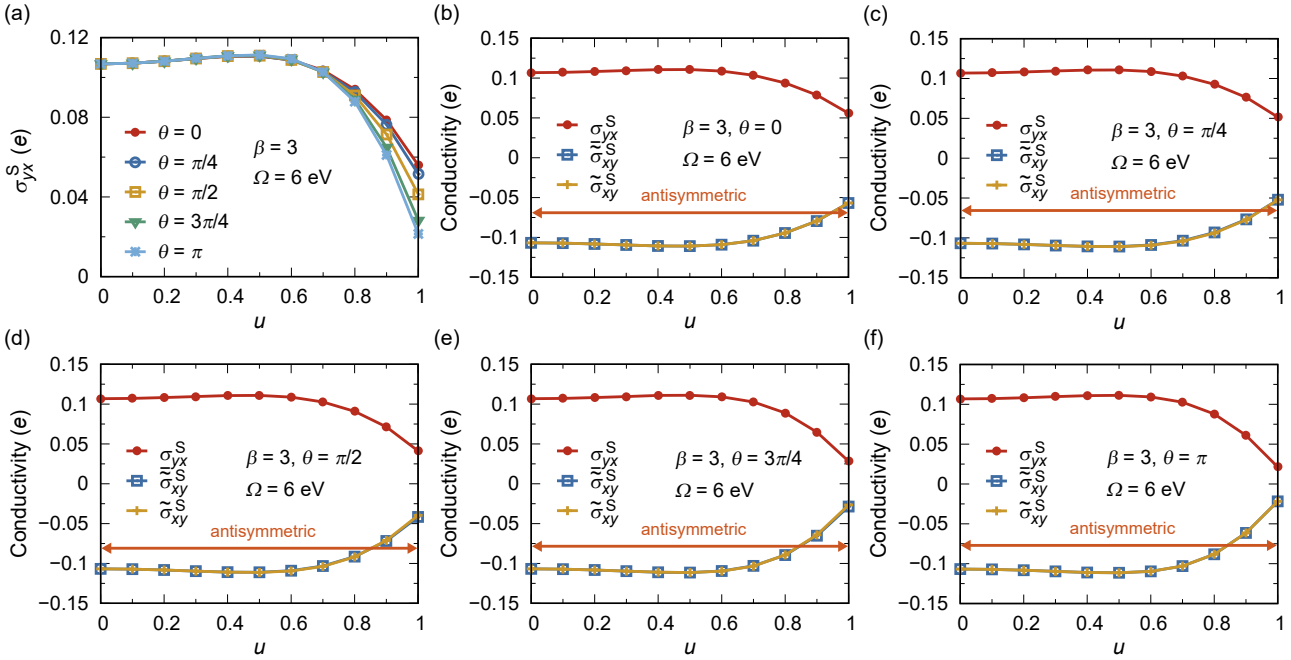

Fig. 9. (Color online) (a) The u ($= eA_0$) dependences of σ^{S}_{yx} for Sr_2RuO_4 driven by BCPL at $\beta = 3$ and $\Omega = 6$ eV with $\theta = 0$, $\frac{\pi}{4}$, $\frac{\pi}{2}$, $\frac{3\pi}{4}$, and π. The pump field of BCPL has been defined in Eqs. (12) and (13). For σ^{S}_{yx}, see Fig. 4(d). The u dependences of σ^{S}_{yx}, $\bar{\tilde{\sigma}}^{S}_{xy}$, and $\tilde{\sigma}^{S}_{xy}$ for Sr_2RuO_4 driven by BCPL at $\beta = 3$ and $\Omega = 6$ eV with (b) $\theta = 0$, (c) $\theta = \frac{\pi}{4}$, (d) $\theta = \frac{\pi}{2}$, (e) $\theta = \frac{3\pi}{4}$, and (f) $\theta = \pi$. For $\bar{\tilde{\sigma}}^{S}_{xy}$ and $\tilde{\sigma}^{S}_{xy}$, see Figs. 4(e) and 4(f), respectively.

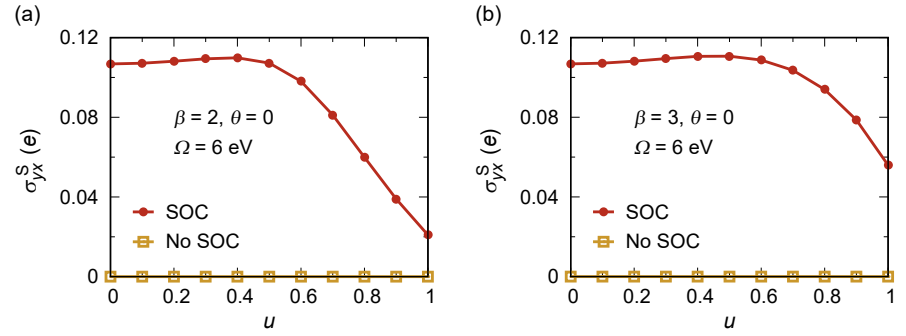

Fig. 10. (Color online) The u ($= eA_0$) dependences of σ^{S}_{yx} for Sr_2RuO_4 driven by BCPL at (a) $\beta = 2$ and (b) $\beta = 3$, $\theta = 0$, and $\Omega = 6$ eV with and without the SOC. Note that in the cases with and without the SOC, $\xi = 0.17$ and 0 eV, respectively.

coupling, as shown in Eq. (27).] This result suggests that the SOC is vital for achieving the finite σ^{S}_{yx}. This is the same as the property for Sr_2RuO_4 driven by CPL.[11] In addition, the same conclusion is obtained with BCPL at $\beta = 3$ and $\theta = 0$, as shown in Fig. 10(b). Therefore, we conclude that the SOC plays the vital role in the SHE of the periodically driven multiorbital metals.

5.2 *Time-averaged charge off-diagonal dc conductivities*

We now compare σ^{C}_{yx}, $\bar{\sigma}^{C}_{xy}$, and σ^{C}_{xy} for Sr_2RuO_4 driven by

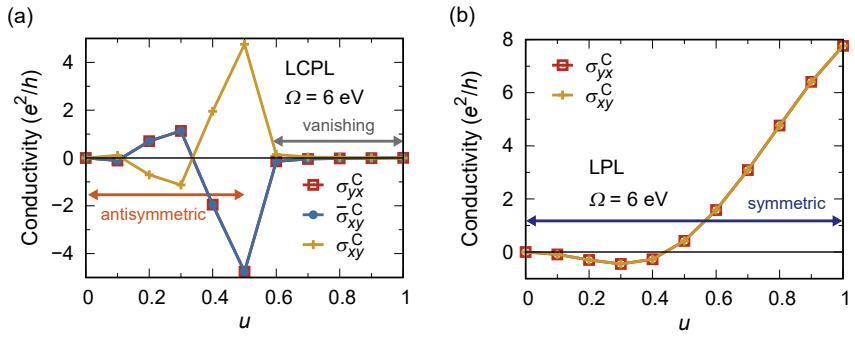

Fig. 11. (Color online) The u ($= eA_0$) dependences of $\sigma^{\rm C}_{yx}$, $\bar{\sigma}^{\rm C}_{xy}$, and $\sigma^{\rm C}_{xy}$ for Sr_2RuO_4 driven by (a) LCPL and (b) LPL at $\Omega = 6$ eV. The pump fields of LCPL and LPL have been defined in Eqs. (4) and (11), respectively. For $\sigma^{\rm C}_{yx}$, $\bar{\sigma}^{\rm C}_{xy}$, and $\sigma^{\rm C}_{xy}$, see Figs. 4(a), 4(b), and 4(c), respectively. In the case with LPL, $\bar{\sigma}^{\rm C}_{xy} = \sigma^{\rm C}_{xy}$.

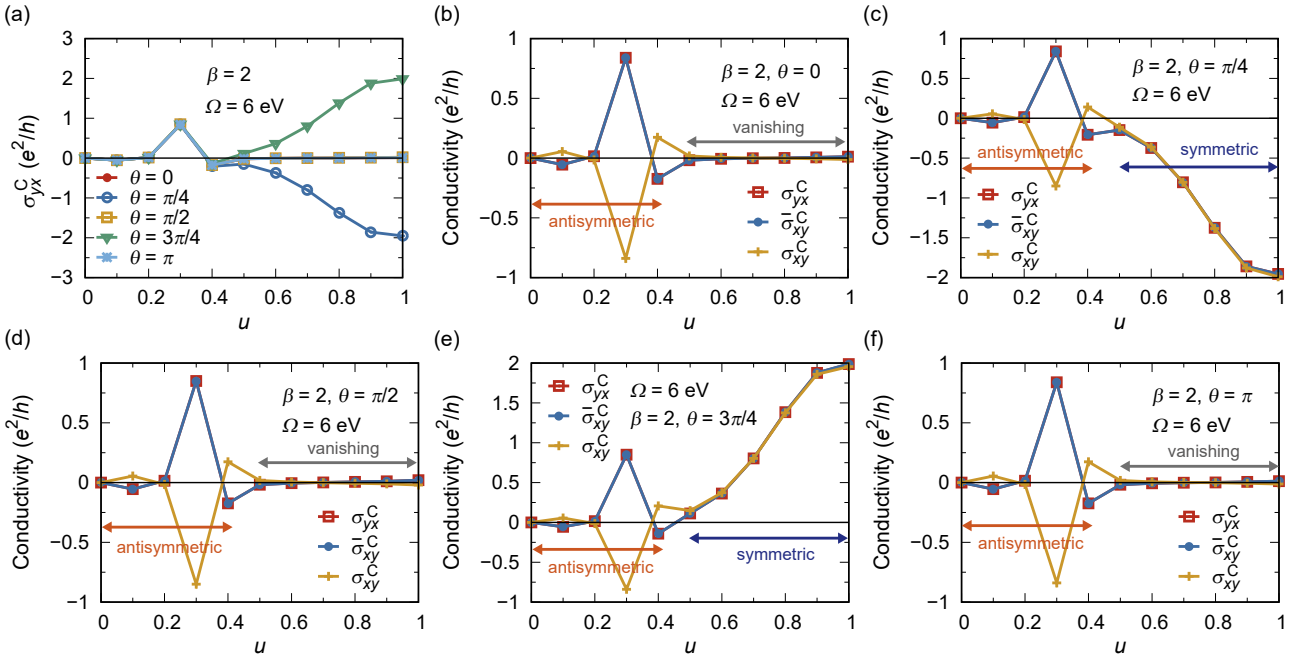

Fig. 12. (Color online) (a) The u ($= eA_0$) dependences of $\sigma^{\rm C}_{yx}$ for Sr_2RuO_4 driven by BCPL at $\beta = 2$ and $\Omega = 6$ eV with $\theta = 0$, $\frac{\pi}{4}$, $\frac{\pi}{2}$, $\frac{3\pi}{4}$, and π. The pump field of BCPL has been defined in Eqs. (12) and (13). For $\sigma^{\rm C}_{yx}$, see Fig. 4(a). The u dependences of $\sigma^{\rm C}_{yx}$, $\bar{\sigma}^{\rm C}_{xy}$, and $\sigma^{\rm C}_{xy}$ for Sr_2RuO_4 driven by BCPL at $\beta = 2$ and $\Omega = 6$ eV with (b) $\theta = 0$, (c) $\theta = \frac{\pi}{4}$, (d) $\theta = \frac{\pi}{2}$, (e) $\theta = \frac{3\pi}{4}$, and (f) $\theta = \pi$. For $\bar{\sigma}^{\rm C}_{xy}$ and $\sigma^{\rm C}_{xy}$, see Figs. 4(b) and 4(c), respectively.

CPL, LPL, or BCPL. In all the cases considered, the Onsager reciprocal relations are satisfied. In addition, in the case with CPL or LPL, $\sigma^{\rm C}_{yx}$ is given by the antisymmetric or symmetric part, respectively. Therefore, $\sigma^{\rm C}_{yx}$ with CPL can be regarded as the anomalous Hall conductivity. Then, in the cases with BCPL at $(\beta, \theta) = (2, \frac{\pi}{4})$, $(2, \frac{3\pi}{4})$, $(3, \frac{\pi}{4})$, $(3, \frac{\pi}{2})$, and $(3, \frac{3\pi}{4})$, the main term is given by the antisymmetric part for small u and by the symmetric part for moderately large u. Meanwhile, in the cases with BCPL at $(\beta, \theta) = (2, 0)$, $(2, \frac{\pi}{2})$, $(2, \pi)$, $(3, 0)$, and $(3, \pi)$, $\sigma^{\rm C}_{yx}$ for moderately large u is almost vanishing, although its main term for small u is given by the antisymmetric part. The unusual crossover between the antisymmetric and symmetric parts may result from the mixture of these parts and the accidentally small value of the antisymmetric part for the moderately strong magnitude of BCPL.

5.2.1 *Case with CPL or LPL*

Figure 11(a) shows the u dependences of $\sigma^{\rm C}_{yx}$, $\bar{\sigma}^{\rm C}_{xy}$, and $\sigma^{\rm C}_{xy}$ for Sr_2RuO_4 driven by LCPL at $\Omega = 6$ eV. Equations (5) and (9), i.e., $\sigma^{\rm C}_{yx} = \bar{\sigma}^{\rm C}_{xy}$ and $\sigma^{\rm C}_{yx} = -\sigma^{\rm C}_{xy}$, hold. These results indicate that $\sigma^{\rm C}_{yx}$ satisfies the Onsager reciprocal relation and is given by the antisymmetric part. This is consistent with the numerical result obtained in graphene driven by CPL.[27)]

Then, Fig. 11(b) shows the u dependences of $\sigma^{\rm C}_{yx}$ and $\sigma^{\rm C}_{xy}$ for Sr_2RuO_4 driven by LPL at $\Omega = 6$ eV. Note that in this case $\bar{\sigma}^{\rm C}_{xy} = \sigma^{\rm C}_{xy}$. In contrast to the case with CPL, $\sigma^{\rm C}_{yx}$ is given by the symmetric part, although it satisfies the Onsager reciprocal relation [i.e., Eq. (10)]. This result also agrees with that obtained in graphene driven by LPL.[27)]

5.2.2 *Cases with BCPL*

Figure 12(a) shows the u dependences of $\sigma^{\rm C}_{yx}$ for Sr_2RuO_4 driven by BCPL at $\beta = 2$ with $\theta = 0$, $\frac{\pi}{4}$, $\frac{\pi}{2}$, $\frac{3\pi}{4}$, and π. $\sigma^{\rm C}_{yx}$ is almost θ-independent in the range of $0 \le u \le 0.4$, whereas it is θ-dependent in the range of $0.5 \le u \le 1$. This θ dependence can be understood in a similar way to the origin of the θ-dependent $\sigma^{\rm S}_{yx}$ (see Sect. 6.1). In contrast to $\sigma^{\rm S}_{yx}$, the magnitude and sign of $\sigma^{\rm C}_{yx}$ can change with increasing u. This may be because the finite $\sigma^{\rm C}_{yx}$ arises from the light-induced

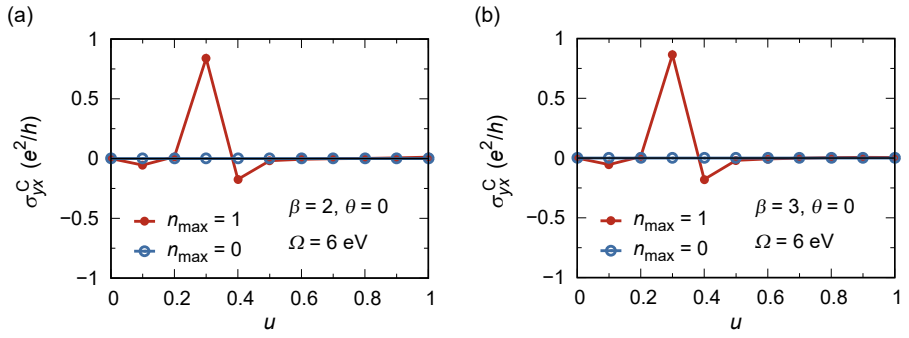

Fig. 13. (Color online) The u ($= eA_0$) dependences of σ^{C}_{yx} for Sr_2RuO_4 driven by BCPL at (a) $\beta = 2$ and (b) $\beta = 3$, $\theta = 0$, and $\Omega = 6$ eV with $n_{max} = 1$ and 0. Here n_{max} is the upper limit of the summation over the Floquet indices (i.e., $\sum_{m,l,n,q=-n_{max}}^{n_{max}}$).

contributions. In fact, $\sigma^{C}_{yx} = 0$ if only the $n_{max} = 0$ terms are considered [Fig. 13(a)].

Figures 12(b)–12(f) compare σ^{C}_{yx}, $\bar{\sigma}^{C}_{xy}$, and σ^{C}_{xy} as functions of u for Sr_2RuO_4 driven by BCPL at $\beta = 2$ with $\theta = 0$, $\frac{\pi}{4}$, $\frac{\pi}{2}$, $\frac{3\pi}{4}$, and π. First, $\sigma^{C}_{yx} = \bar{\sigma}^{C}_{xy}$ holds at these θ's. Namely, the Onsager reciprocal relation Eq. (14) is numerically validated. Then, at $\theta = 0$, $\frac{\pi}{2}$, and π, σ^{C}_{yx} for $u \leq 0.4$ is dominated by the antisymmetric part, whereas σ^{C}_{yx} for moderately larger u is almost vanishing. Meanwhile, at $\theta = \frac{\pi}{4}$ and $\frac{3\pi}{4}$, the antisymmetric part is the main term of σ^{C}_{yx} for $u \leq 0.4$, but the symmetric part becomes the main term for larger u. This suggests that for Sr_2RuO_4 driven by BCPL at $\beta = 2$ with some θ's, the main term of σ^{C}_{yx} can be changed from the antisymmetric part to the symmetric part or vice versa by tuning the magnitude of the pump field of BCPL. This unusual crossover may be surprising, but it does not contradict the Onsager reciprocal relation because this relation with BCPL cannot be reduced to the antisymmetric or symmetric part in general (see Sect. 2.1.2).

The above crossover might be due to the mixture of the antisymmetric and symmetric parts and the vanishingly small antisymmetric part for large u. As we can see from Figs. 12(a) and 12(b), the θ-independent terms of σ^{C}_{yx} are finite and dominated by the antisymmetric part in the range of $0 \leq u \leq 0.4$, whereas they become almost vanishing in the range of $0.5 \leq u \leq 1$. In addition, as we can see from Figs. 12(a) and 12(c)–12(f), the θ-dependent terms become non-negligible only in the range of $0.5 \leq u \leq 1$ and are dominated by the symmetric part. These results imply that the crossover between the antisymmetric and symmetric parts with changing u might arise from a combination of the mixture of these parts and the accidentally small antisymmetric part in the range of $0.5 \leq u \leq 1$. As we have explained in Sect. 2.1.2, the Onsager reciprocal relation with BCPL does not exclude a possibility of such a mixture. In fact, such a mixture can be realized in another periodically driven system with BCPL,[30] although the antisymmetric part is dominant for all the u's in the range of $0 \leq u \leq 1$. We should note that the accidentally small antisymmetric part may be characteristic of this model, but its origin is difficult to be clarified.

The symmetric relation between σ^{C}_{yx}'s at a couple of θ's for moderately large u could be understood in terms of the symmetry of $\mathbf{A}_{BCPL}(t)$. Figure 12(a) or 14(a) shows that σ^{C}_{yx}'s at $\theta = \frac{\pi}{4}$ and $\frac{3\pi}{4}$ at a certain u in the range of $0.5 \leq u \leq 1$ are of almost the same magnitude and of opposite sign. This may be characteristic of the symmetric part of σ^{C}_{yx} because σ^{C}_{yx} in the range of $0.5 \leq u \leq 1$ is dominated by the symmetric part [Figs. 12(c) and 12(e)]. The similar property is achieved in graphene driven by LPL if σ^{C}_{yx}'s with the pump fields of LPL connected by a mirror operation are compared.[27] As we can see from Fig. 14(d), the trajectories of $\mathbf{A}_{BCPL}(t)$'s at $\theta = \frac{\pi}{4}$ and $\frac{3\pi}{4}$ are connected by a mirror operation about the $A_x = 0$ plane. Therefore, the symmetric relation between σ^{C}_{yx}'s at $\theta = \frac{\pi}{4}$ and $\frac{3\pi}{4}$ in the range of $0.5 \leq u \leq 1$ could be linked to the mirror symmetry of the trajectories of $\mathbf{A}_{BCPL}(t)$'s. This interpretation remains valid even if we compare σ^{C}_{yx}'s at $\theta = \frac{\pi}{4}$ and $-\frac{\pi}{4}$ [Fig. 14(b)] or at $\theta = \frac{3\pi}{4}$ and $\frac{5\pi}{4}$ [Fig. 14(c)] in the range of $0.5 \leq u \leq 1$. The trajectories at $\theta = \frac{\pi}{4}$ and $-\frac{\pi}{4}$ or at $\theta = \frac{3\pi}{4}$ and $\frac{5\pi}{4}$ are connected by another mirror operation about the $A_y = 0$ plane [see Figs. 14(e) and 14(f)].

The similar properties hold at $\beta = 3$. First, σ^{C}_{yx} is almost independent of θ in the range of $0 \leq u \leq 0.4$ and dependent on it in the range of $0.5 \leq u \leq 1$ [see Fig. 15(a)]. Second, the light-induced terms are vital for achieving the finite σ^{C}_{yx} [see Fig. 13(b)]. Third, the Onsager reciprocal relation $\sigma^{C}_{yx} = \bar{\sigma}^{C}_{xy}$ holds at $\theta = 0$, $\frac{\pi}{4}$, $\frac{\pi}{2}$, $\frac{3\pi}{4}$, and π [see Figs. 15(b)–15(f)]. Fourth, σ^{C}_{yx} in the range of $0 \leq u \leq 0.4$ is dominated by the antisymmetric part at these θ's, whereas σ^{C}_{yx} in the range of $0.5 \leq u \leq 1$ is almost vanishing at $\theta = 0$ and π and dominated by the symmetric part at $\frac{\pi}{4}$, $\frac{\pi}{2}$, and $\frac{3\pi}{4}$ [see Figs. 15(b)–15(f)]. Fifth, σ^{C}_{yx}'s at $\theta = \frac{\pi}{2}$ and $\frac{3\pi}{2}$, at $\theta = \frac{\pi}{4}$ and $\frac{7\pi}{4}$, or at $\theta = \frac{3\pi}{4}$ and $\frac{5\pi}{4}$ in the range of $0.5 \leq u \leq 1$ are of almost the same magnitude and of opposite sign [see Figs. 16(a)–16(c)]; and the trajectories of $\mathbf{A}_{BCPL}(t)$'s at each couple are connected by the mirror operation about the $A_x = 0$ or $A_y = 0$ plane [see Figs. 16(d)–16(f)].

Finally, we remark on the role of the SOC. Figures 17(a) and 17(b) show the u dependences of σ^{C}_{yx} without SOC for Sr_2RuO_4 driven by BCPL at $\beta = 2$ and 3, respectively, with $\theta = 0$, $\frac{\pi}{4}$, $\frac{\pi}{2}$, $\frac{3\pi}{4}$, and π. Comparing Figs. 17(a) and 12(a) or Figs. 17(b) and 15(a), we find that the effect of the SOC on σ^{C}_{yx} is not large. In particular, σ^{C}_{yx} can be finite even without the SOC. This is in contrast to the vital role of the SOC in σ^{S}_{yx} and similar to the property obtained in Sr_2RuO_4 driven by CPL.[11] These results suggest that the SOC is not important in discussing σ^{C}_{yx} of the periodically driven multiorbital metals.

6. Discussion

6.1 *Origin of the θ dependences of σ^{S}_{yx} and σ^{C}_{yx}*

First, we discuss the origin of the θ dependences of σ^{S}_{yx} and σ^{C}_{yx} for Sr_2RuO_4 driven by BCPL at $\beta = 2$ and 3. As we have

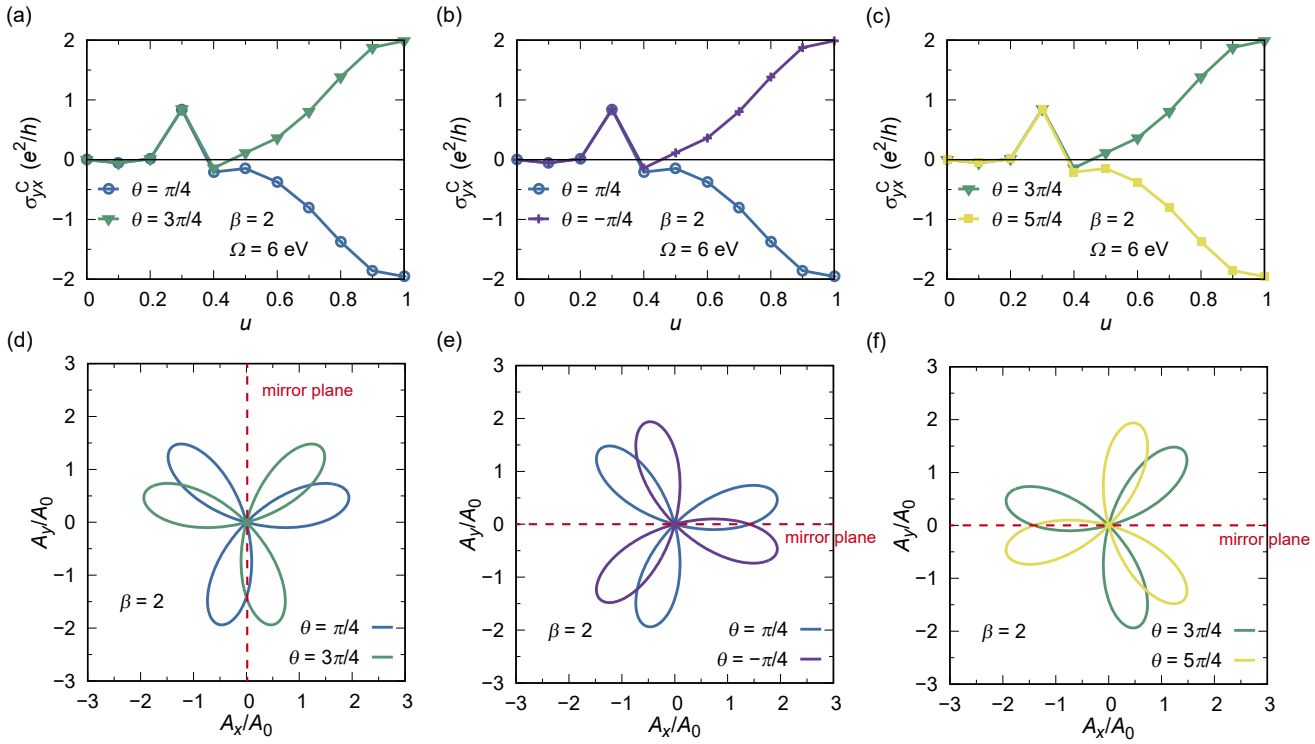

Fig. 14. (Color online) The u ($= eA_0$) dependences of $\sigma^{\rm C}_{yx}$ for Sr_2RuO_4 driven by BCPL at $\beta = 2$ and $\Omega = 6$ eV with (a) $\theta = \frac{\pi}{4}$ and $\frac{3\pi}{4}$, (b) $\theta = \frac{\pi}{4}$ and $-\frac{\pi}{4}$, and (c) $\theta = \frac{3\pi}{4}$ and $\frac{5\pi}{4}$. The trajectories of the pump fields of BCPL per period $T_{\rm p}$ at $\beta = 2$ with (d) $\theta = \frac{\pi}{4}$ and $\frac{3\pi}{4}$, (e) $\theta = \frac{\pi}{4}$ and $-\frac{\pi}{4}$, and (f) $\theta = \frac{3\pi}{4}$ and $\frac{5\pi}{4}$. The two trajectories in panel (d) are connected by the mirror operation about the $A_x = 0$ plane, whereas those in panel (e) or (f) are connected by the mirror operation about the $A_y = 0$ plane.

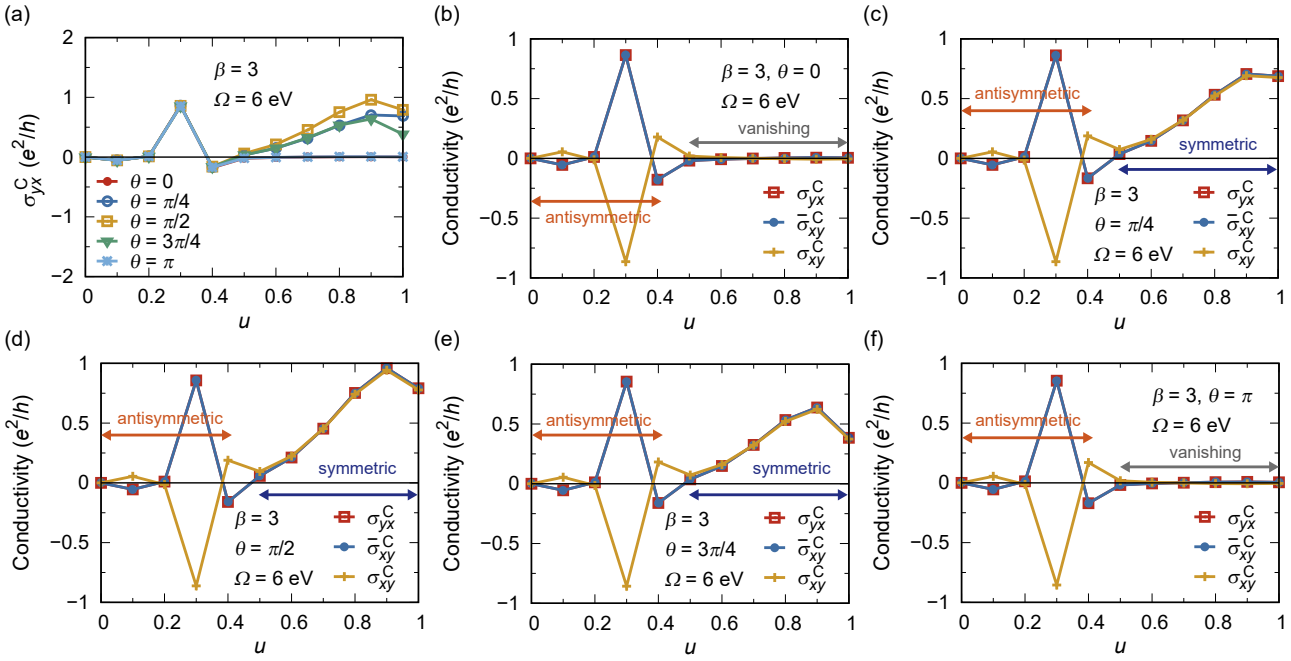

Fig. 15. (Color online) (a) The u ($= eA_0$) dependences of $\sigma^{\rm C}_{yx}$ for Sr_2RuO_4 driven by BCPL at $\beta = 3$ and $\Omega = 6$ eV with $\theta = 0, \frac{\pi}{4}, \frac{\pi}{2}, \frac{3\pi}{4}$, and π. A_0, β, and θ of BCPL have been defined in Eqs. (12) and (13). For $\sigma^{\rm C}_{yx}$, see Fig. 4(a). The u dependences of $\sigma^{\rm C}_{yx}$, $\bar{\sigma}^{\rm C}_{xy}$, and $\sigma^{\rm C}_{xy}$ for Sr_2RuO_4 driven by BCPL at $\beta = 3$ and $\Omega = 6$ eV with (b) $\theta = 0$, (c) $\theta = \frac{\pi}{4}$, (d) $\theta = \frac{\pi}{2}$, (e) $\theta = \frac{3\pi}{4}$, and (f) $\theta = \pi$. For $\bar{\sigma}^{\rm C}_{xy}$ and $\sigma^{\rm C}_{xy}$, see Figs. 4(b) and 4(c), respectively.

shown in Figs. 7(a), 9(a), 12(a), and 15(a), $\sigma^{\rm S}_{yx}$ and $\sigma^{\rm C}_{yx}$ are almost independent of θ for small u, whereas they depend on θ for moderately large u. This property could be understood by discussing the u and θ dependences of the kinetic energy terms $[\epsilon_{ab}(\mathbf{k})]_{mn}$'s because the effects of $\mathbf{A}_{\rm BCPL}(t)$ are taken into account via the Peierls phase factor in the kinetic energy [see Eqs. (33) and (73)]. Let us consider $[\epsilon_{d_{yz}d_{yz}}(\mathbf{k})]_{mn}$ for example. As shown in Appendix B, $[\epsilon_{d_{yz}d_{yz}}(\mathbf{k})]_{mn}$ is given by

$$[\epsilon_{d_{yz}d_{yz}}(\mathbf{k})]_{mn} = -t_2 I^{mn}_x(k_x, u, \theta, \beta) - t_1 I^{mn}_y(k_y, u, \theta, \beta), \quad (89)$$

where

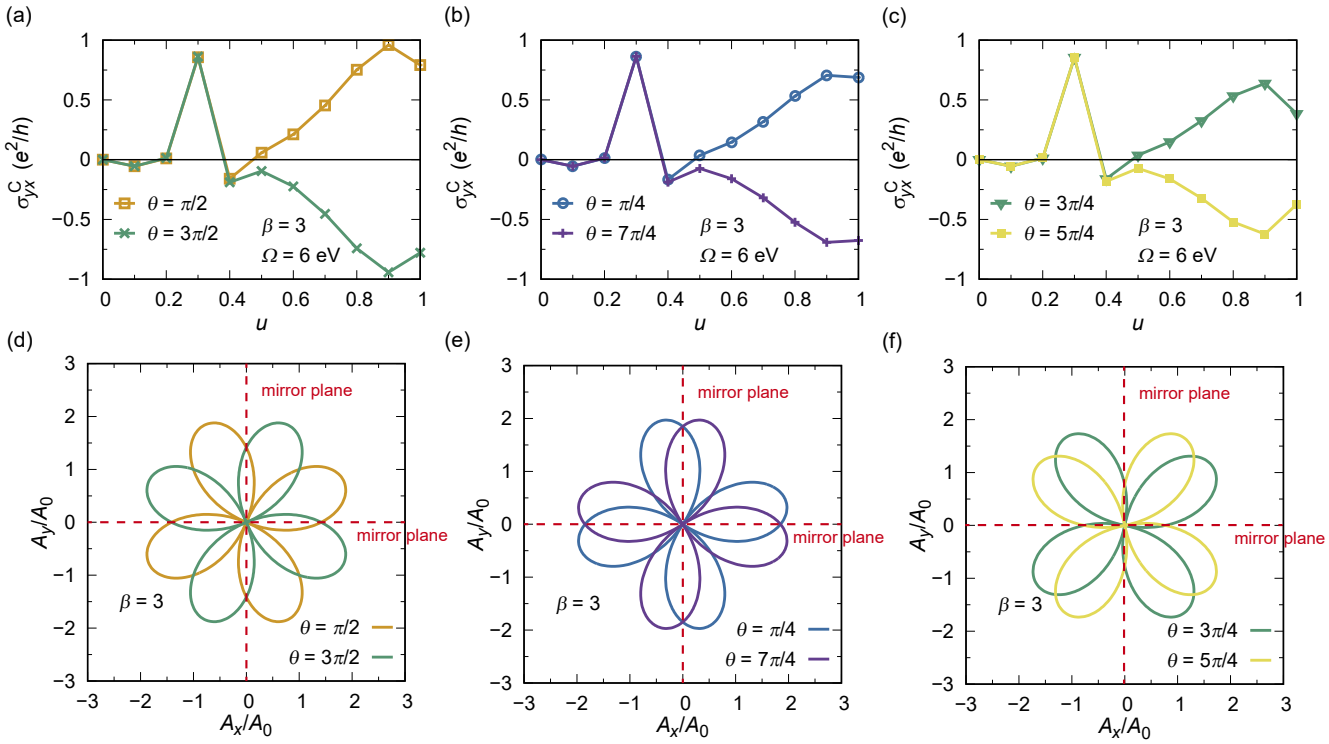

Fig. 16. (Color online) The u ($= eA_0$) dependences of σ^{C}_{yx} for Sr_2RuO_4 driven by BCPL at $\beta = 3$ and $\Omega = 6$ eV with (a) $\theta = \frac{\pi}{2}$ and $\frac{3\pi}{2}$, (b) $\theta = \frac{\pi}{4}$ and $\frac{7\pi}{4}$, and (c) $\theta = \frac{3\pi}{4}$ and $\frac{5\pi}{4}$. The trajectories of the pump fields of BCPL per period T_p at $\beta = 3$ with (d) $\theta = \frac{\pi}{2}$ and $\frac{3\pi}{2}$, (e) $\theta = \frac{\pi}{4}$ and $\frac{7\pi}{4}$, and (f) $\theta = \frac{3\pi}{4}$ and $\frac{5\pi}{4}$. The two trajectories in each panel are connected by the mirror operation about the $A_x = 0$ or $A_y = 0$ plane.

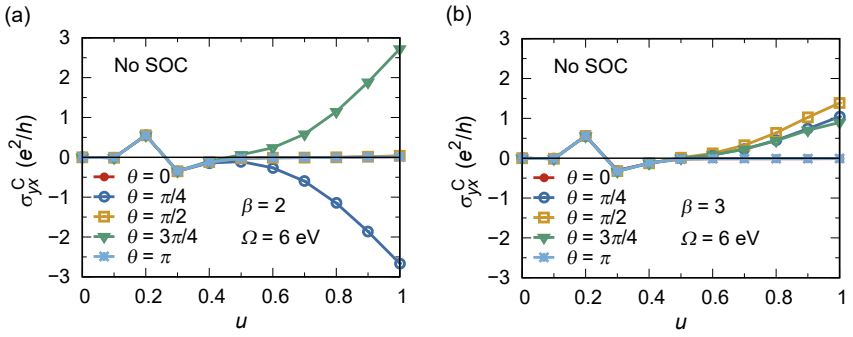

Fig. 17. (Color online) The u ($= eA_0$) dependences of σ^{C}_{yx} for Sr_2RuO_4 driven by BCPL at (a) $\beta = 2$ and (b) $\beta = 3$ and $\Omega = 6$ eV with $\theta = 0$, $\frac{\pi}{4}$, $\frac{\pi}{2}$, $\frac{3\pi}{4}$, and π in the absence of SOC.

$$I_x^{mn}(k_x, u, \theta, \beta) = \sum_{l=-\infty}^{\infty} i^{n-m-(\beta-1)l} e^{-il\theta} \mathcal{J}_{n-m-\beta l}(u) \mathcal{J}_l(u) [e^{-ik_x}(-1)^{n-m-(\beta-1)l} + e^{ik_x}], \tag{90}$$

$$I_y^{mn}(k_y, u, \theta, \beta) = \sum_{l=-\infty}^{\infty} e^{-il\theta}(-1)^l \mathcal{J}_{n-m-\beta l}(u) \mathcal{J}_l(u) [e^{-ik_y}(-1)^{n-m-(\beta-1)l} + e^{ik_y}], \tag{91}$$

and $\mathcal{J}_l(u)$ is the lth-order Bessel function of the first kind. For simplicity, we restrict the Floquet indices m, n, and l to be $-1 \le m, n, l \le 1$, which corresponds to the case at $n_{\max} = 1$. After some calculation, we obtain $I_x^{mn}(k_x, u, \theta, \beta)$'s at $\beta = 2$ and 3,

$$\begin{aligned} I_x^{mn}(k_x, u, \theta, 2) \sim\ & 2\delta_{n-m,0} \cos k_x \mathcal{J}_0(u)^2 - 2(\delta_{n-m,1} + \delta_{n-m,-1}) \sin k_x \mathcal{J}_0(u) \mathcal{J}_1(u) \\ & - 2(e^{-i\theta}\delta_{n-m,1} + e^{i\theta}\delta_{n-m,-1}) \cos k_x \mathcal{J}_1(u)^2 \\ & - 2(\delta_{n-m,2} + \delta_{n-m,-2}) \cos k_x \mathcal{J}_0(u) \mathcal{J}_2(u) \\ & - 2(e^{-i\theta}\delta_{n-m,2} + e^{i\theta}\delta_{n-m,-2}) \sin k_x \mathcal{J}_0(u) \mathcal{J}_1(u) + O(u^3), \end{aligned} \tag{92}$$

and

$$\begin{aligned} I_x^{mn}(k_x, u, \theta, 3) \sim\ & 2\delta_{n-m,0} \cos k_x \mathcal{J}_0(u)^2 - 2(\delta_{n-m,1} + \delta_{n-m,-1}) \sin k_x \mathcal{J}_0(u) \mathcal{J}_1(u) \\ & - 2(\delta_{n-m,2} + \delta_{n-m,-2}) \cos k_x \mathcal{J}_0(u) \mathcal{J}_2(u) \\ & - 2(e^{-i\theta}\delta_{n-m,2} + e^{i\theta}\delta_{n-m,-2}) \cos k_x \mathcal{J}_1(u)^2 + O(u^3). \end{aligned} \tag{93}$$

These equations show that the θ dependences arise from the light-induced corrections due to the finite-order Bessel functions. Note that $I_y^{mn}(k_y, u, \theta, \beta)$'s at $\beta = 2$ and 3 have the same property. By using the series expansions of the Bessel functions, we can express Eqs. (92) and (93) as follows:

$$\begin{aligned} I_x^{mn}(k_x, u, \theta, 2) \sim\ & \delta_{n-m,0}(2-u^2)\cos k_x - (\delta_{n-m,1} + \delta_{n-m,-1})u \sin k_x \\ & - (e^{-i\theta}\delta_{n-m,1} + e^{i\theta}\delta_{n-m,-1})\frac{u^2}{2}\cos k_x \\ & - (\delta_{n-m,2} + \delta_{n-m,-2})\frac{u^2}{4}\cos k_x \\ & - (e^{-i\theta}\delta_{n-m,2} + e^{i\theta}\delta_{n-m,-2})u \sin k_x + O(u^3), \end{aligned} \tag{94}$$

and

$$\begin{aligned} I_x^{mn}(k_x, u, \theta, 3) \sim\ & \delta_{n-m,0}(2-u^2)\cos k_x - (\delta_{n-m,1} + \delta_{n-m,-1})u \sin k_x \\ & - (\delta_{n-m,2} + \delta_{n-m,-2})\frac{u^2}{4}\cos k_x \\ & - (e^{-i\theta}\delta_{n-m,2} + e^{i\theta}\delta_{n-m,-2})\frac{u^2}{2}\cos k_x + O(u^3). \end{aligned} \tag{95}$$

These equations can explain the θ-independent σ_{yx}^{S} for small u because the terms for $n - m = 0$ are primary (if they give the finite contribution). Although the terms for $n - m \neq 0$ are necessary for $\sigma_{yx}^{\mathrm{C}} \neq 0$, these equations can also explain the θ-independent σ_{yx}^{C} for small u, at which the terms for $n - m = \pm 1$ are dominant. This is because in the small-u region, the θ-independent u^1 terms are more important than the θ-dependent u^2 terms. For moderately large u, the θ-dependent u^2 terms for $n - m = \pm 1$ may become non-negligible. Therefore, the θ dependences of σ_{yx}^{S} and σ_{yx}^{C} could be interpreted in terms of the u and θ dependences of the light-induced corrections to the kinetic energy.

6.2 *Comparisons with other relevant studies*

We now compare our results about the Onsager reciprocal relations with other relevant studies. As described in Sect. 1, there are several studies[24–27] about the Onsager reciprocal relations in periodically driven systems. In two of them,[24,25] the time-periodic field was treated as perturbation. Meanwhile, in our theory, the time-periodic pump field has been treated nonperturbatively. In general, the time-periodic field should be treated nonperturbatively to describe periodically driven systems because its nonperturbative effects often change the electronic states drastically. Therefore, the systems studied in these papers[24,25] are insufficient to discuss the standard periodically driven systems. Then, in another,[26] the Onsager reciprocal relations about the matter or energy transport between a periodically driven system and one of the three reservoirs were studied. This is distinct from the transport phenomena within periodically driven systems. Therefore, except our previous paper,[27] there has been no study of the Onsager reciprocal relations for any transport within periodically driven systems in which the nonperturbative effects of the driving field are taken into account. In that paper,[27] we numerically studied the time-averaged charge off-diagonal dc conductivities σ_{yx}^{C} and σ_{xy}^{C} in graphene driven by CPL or LPL and found that $\sigma_{yx}^{\mathrm{C}} = -\sigma_{xy}^{\mathrm{C}}$ or $\sigma_{yx}^{\mathrm{C}} = \sigma_{xy}^{\mathrm{C}}$ holds with CPL or LPL, respectively. However, we did not discuss the generality of these relations, i.e., we just showed that they are satisfied in our numerical results. Meanwhile, in this paper, we have made general arguments about the Onsager reciprocal relations for spin and charge transport within the periodically driven systems. These arguments are applicable to many periodically driven systems and extendable to others. Therefore, this work is the first systematic study of the Onsager reciprocal relations in periodically driven systems. Most importantly, this paper is the first work demonstrating the Onsager reciprocal relations for the spin transport in periodically driven systems.

Next, we compare our results in the case of BCPL at $\beta = 3$ with our previous study[30] for graphene driven by BCPL at $\beta = 3$. (Although we have also studied the case at $\beta = 2$ there,[30] its results are not directly comparable to the results obtained in this paper due to the vital role of the valley degree of freedom in that case studied in Ref. 30.) There are three similarities between our results shown in Sect. 5.2.2 and those obtained in this previous study:[30] σ_{yx}^{C} is almost independent of θ for small u and depends on it for moderately large u; σ_{yx}^{C} for small u is dominated by the antisymmetric part; and the antisymmetric and symmetric parts are mixed for moderately large u at $\theta = \frac{\pi}{2}$. Therefore, these properties may be characteristic properties of σ_{yx}^{C} in systems driven by BCPL. Then, the difference is that the antisymmetric part of σ_{yx}^{C} becomes almost vanishing for moderately large u in Sr_2RuO_4 driven by BCPL at $\theta = 0$ and π, whereas the antisymmetric part remains dominant even for moderately large u in graphene driven by BCPL at these θ's.[30]

We turn to the comparisons with some theoretical studies[66–68] about transport properties with BCPL at $\beta = 2$. In these studies, the effects of the BCPL on charge or spin transport have been analyzed in perturbation theories. First, our results about the effects of the SOC are similar to those on the charge and spin conductivities of another three-orbital electron system having the z component of the SOC in the second-order perturbation theory against the BCPL field.[67] This similarity may be reasonable because the SOC is treated nonperturbatively in both cases. Then, our θ-dependent σ_{yx}^{C} is similar to the θ-dependent charge conductivity obtained in the third-order perturbation theory against the BCPL field.[68] However, a critical value of u above which σ_{yx}^{C} depends on θ exists only in our case [see Fig. 12(a)]. This critical value may arise from the nonlinear u terms of the light-induced corrections, as we have discussed in Sect. 6.1. Therefore, the crossover between the θ-independent and θ-dependent σ_{yx}^{C}

may be characteristic of nonperturbative effects of BCPL. This interpretation remains valid in graphene driven by BCPL.[30] Although the authors of Ref. 68 have claimed that a nonperturbative effect is also discussed, their discussions are insufficient because they have used an approximation for the Hamiltonian, $H_0[k + A(t)] \approx H_0(k) + A(t)\frac{\partial H_0(k)}{\partial k}$ [see Eq. (29) of Supplemental Material of Ref. 68], which is valid only if $A(t)$, the vector potential of the BCPL, can be treated perturbatively. Namely, their theory can analyze only the perturbative effects of the BCPL. We do not use such an approximation; instead, we have analyzed the nonperturbative effects of BCPL in the standard Floquet linear-response theory.[8,11,38,49]

6.3 *Experimental realization*

Finally, we comment on experimental realization of our results. We have supposed that our periodically driven open system can reach a nonequilibrium steady state due to the damping Γ. The AHE predicted in such a periodically driven open system[7] was experimentally observed.[10] Therefore, our time-averaged charge off-diagonal dc conductivities could be experimentally observed in the pump-probe measurements for periodically driven Sr_2RuO_4. In addition, our SHE could be detected via the inverse SHE[22,23] because we have demonstrated that σ^{S}_{yx} satisfies the Onsager reciprocal relation, which is similar to that in nondriven systems, and is dominated by the antisymmetric part. Note that $\tilde{\sigma}^{\mathrm{S}}_{xy}$ could be experimentally observed by measuring the charge current perpendicular to the probe spin field [see Fig. 4(f)]. As the probe spin field, we can use, for example, the gradient of the Zeeman field, which could be experimentally realized.[69] In the case of Sr_2RuO_4, $u = 0.1$ for $\Omega = 6\,\mathrm{eV}$ corresponds to $E_0 \approx 15.4\,\mathrm{MV/cm}$, where we have used $u = ea_{\mathrm{NN}}A_0 = ea_{\mathrm{NN}}E_0/\Omega$ and $a_{\mathrm{NN}} \approx 0.39\,\mathrm{nm}$.[70] From an experimental point of view, the pump field of the order of $10\,\mathrm{MV/cm}$ can be realized.[71] Therefore, it may be possible to observe the θ-dependent σ^{C}_{yx} and σ^{S}_{yx} for moderately large u as well as the θ-independent σ^{C}_{yx} and σ^{S}_{yx} for small u. Although there is a possibility that the similar θ-dependent σ^{C}_{yx} and σ^{S}_{yx} will be realized even for smaller Ω and E_0, it is difficult to check this possibility due to the huge cost of the numerical calculations. Note that in the case of CPL,[11] the u dependence of the σ^{S}_{yx} or σ^{C}_{yx} obtained for $\Omega = 6\,\mathrm{eV}$ is similar to that obtained for smaller Ω.

7. Conclusions

In summary, we have theoretically established the Onsager reciprocal relations for the charge and spin transport in the periodically driven systems. We have made general arguments about these relations for σ^{C}_{yx} and σ^{S}_{yx} in the periodically driven systems with CPL, LPL, and BCPL. We have shown that σ^{C}_{yx} and σ^{S}_{yx} satisfy the Onsager reciprocal relations in all the cases considered and that their main terms depend on the polarization of light. In the case with CPL or LPL, σ^{C}_{yx} is dominated by the antisymmetric or symmetric part, respectively, whereas σ^{S}_{yx} is dominated by the antisymmetric part. Meanwhile, in the case with BCPL, σ^{C}_{yx} and σ^{S}_{yx} are not restricted to either the antisymmetric or symmetric part generally. Then, we have numerically analyzed σ^{C}_{yx}, σ^{S}_{yx}, and the other time-averaged off-diagonal dc conductivities appearing in the Onsager reciprocal relations by applying the Floquet linear-response theory to the model of periodically driven Sr_2RuO_4. We have demonstrated the validity of our arguments. In addition, we have shown in the cases with BCPL that the main term of σ^{S}_{yx} is given by the antisymmetric part, whereas that of σ^{C}_{yx} depends on the magnitude of the pump field. More precisely, σ^{C}_{yx} for small u is dominated by the antisymmetric part, whereas σ^{C}_{yx} for moderately large u is almost vanishing or dominated by the symmetric part.

Our arguments and numerical calculations have demonstrated that σ^{S}_{yx} in the periodically driven systems satisfies the Onsager reciprocal relation. This means that the finite σ^{S}_{yx} in the periodically driven systems can be indirectly observed by measuring the time-averaged dc conductivity of the inverse SHE. Therefore, our results open the way for detecting the spin current in periodically driven systems via the inverse SHE. Since such an indirect detection method has been widely used in many spintronics phenomena of nondriven systems,[72] this achievement is useful to develop and observe many spintronics phenomena in periodically driven systems. Therefore, our results provide a vital step towards comprehensive understanding and further development of spintronics in periodically driven systems.

Our arguments have shown an essential difference between the Onsager reciprocal relations for σ^{C}_{yx} and σ^{S}_{yx}. The difference is that σ^{C}_{yx} possesses the antisymmetric part only without time-reversal symmetry, whereas σ^{S}_{yx} possesses the antisymmetric part even with it. This is consistent with the fact that the AHE is possible with broken time-reversal symmetry, whereas the SHE is possible even with time-reversal symmetry. This difference is due to the difference between the time-reversal symmetries of the charge and spin currents.

Moreover, our arguments have resolved the contradictory statements about the Onsager reciprocal relation for the spin transport in nondriven systems.[34–37] There is a previous study claiming the violation of the Onsager reciprocal relation for the spin transport,[36] whereas there are other studies claiming its existence.[34,35,37] Furthermore, among the latter studies, the expression of the Onsager reciprocal relation is different: in one of them[35] the spin off-diagonal dc conductivity is dominated by the symmetric part, whereas in the others[34,37] it is dominated by the antisymmetric part. As we have shown in Sect. 2.2.1, our results are consistent with the results of the last two studies,[34,37] i.e., the spin off-diagonal dc conductivity satisfies the Onsager reciprocal relation even with time-reversal symmetry and is dominated by the antisymmetric part. Therefore, our arguments support the validity of the interpretation of the inverse SHE[22,23] as the existence of the spin current in nondriven systems.

Then, our numerical calculations in the cases with BCPL have indicated that σ^{C}_{yx} cannot necessarily be regarded as the anomalous Hall conductivity even if time-reversal symmetry is broken. In general, we can regard σ^{C}_{yx} as the anomalous Hall conductivity if and only if σ^{C}_{yx} is dominated by the antisymmetric part. In addition, time-reversal symmetry can be broken by BCPL.[30] As shown in Sect. 5.2.2, σ^{C}_{yx} with BCPL for moderately large u is almost vanishing or dominated by the symmetric part, although that for small u is dominated by the antisymmetric part. This unusual property does not contradict the Onsager reciprocal relation because this relation in the case with BCPL restricts σ^{C}_{yx} to

neither the antisymmetric nor symmetric part generally (see Sect. 2.1.2). It may be due to the lack of a simple relation between the pump field of BCPL and its time-reversal counterpart. In contrast, the pump field of CPL has the simple relation $\mathbf{A}_{\mathrm{LCPL}}(-t) = \mathbf{A}_{\mathrm{RCPL}}(t)$; as a result, σ^{C}_{yx} with CPL is restricted to the antisymmetric part (see Sect. 2.1.2). These results suggest that even if time-reversal symmetry can be broken by the pump field, it is highly required to check whether or not the main term of σ^{C}_{yx} is given by the antisymmetric part in discussing the AHE. It is also necessary to check the main term of σ^{S}_{yx} to discuss the SHE because in some cases such as the cases with BCPL its main term is not restricted by the Onsager reciprocal relation to either the antisymmetric or symmetric part. These suggestions are useful for future studies of the AHE and SHE.

This paper will stimulate many future studies of transport phenomena in periodically driven systems. First, our results allow the experimental detection of the spin current in periodically driven systems via the inverse SHE. The impact of our paper is not restricted to the SHE, but it will encourage future studies of other spintronics phenomena such as the spin Seebeck effect[72–75] in periodically driven systems. This is because the inverse SHE is often used to convert the spin current into an electrical signal. Then, our results will provide a useful guideline when studying the Onsager reciprocal relations for the time-averaged charge and spin off-diagonal dc conductivities in the systems driven by CPL, LPL, or BCPL. Moreover, our general arguments and theory can be extended to the other transport coefficients including the ac conductivities in periodically driven systems. The extension to the transport coefficients in the non-linear regime is also an important future study.

Acknowledgments This work was supported by JST CREST Grant No. JPMJCR1901, JSPS KAKENHI Grant No. JP22K03532, and MEXT Q-LEAP Grant No. JP-MXS0118067426.

Appendix A: Derivation of Eq. (55)

We derive Eq. (55). Since we have explained this derivation in Ref. 11, we here describe its main points. Substituting Eq. (42) or (43) into Eq. (52), we obtain

$$\sigma^{\mathrm{Q}}_{yx}(\omega) = \mathrm{Re}[\sigma^{\mathrm{Q}(1)}_{yx}(\omega) + \sigma^{\mathrm{Q}(2)}_{yx}(\omega)], \tag{A·1}$$

where

$$\sigma^{\mathrm{Q}(1)}_{yx}(\omega) = \int_0^{T_{\mathrm{p}}} \frac{dt_{\mathrm{av}}}{T_{\mathrm{p}}} \int_{-\infty}^{\infty} dt_{\mathrm{rel}}\, e^{i\omega t_{\mathrm{rel}}} \sigma^{\mathrm{Q}(1)}_{yx}\left(t_{\mathrm{av}} + \frac{t_{\mathrm{rel}}}{2}, t_{\mathrm{av}} - \frac{t_{\mathrm{rel}}}{2}\right), \tag{A·2}$$

$$\sigma^{\mathrm{Q}(2)}_{yx}(\omega) = \int_0^{T_{\mathrm{p}}} \frac{dt_{\mathrm{av}}}{T_{\mathrm{p}}} \int_{-\infty}^{\infty} dt_{\mathrm{rel}}\, e^{i\omega t_{\mathrm{rel}}} \sigma^{\mathrm{Q}(2)}_{yx}\left(t_{\mathrm{av}} + \frac{t_{\mathrm{rel}}}{2}, t_{\mathrm{av}} - \frac{t_{\mathrm{rel}}}{2}\right). \tag{A·3}$$

We calculate the right-hand sides of Eqs. (A·2) and (A·3) using Eqs. (44) and (50), the Floquet representation of the Green's functions, and two relations. One of the two relations is that the Floquet representation of a function $A(t,t') = \int dt''\, B(t,t'')C(t'',t')$ is given by

$$[A(\omega)]_{mn} = \sum_{l=-\infty}^{\infty} [B(\omega)]_{ml}[C(\omega)]_{ln}. \tag{A·4}$$

The other is that a product $a(t)D(t,t')$ is expressed in the Floquet representation as

$$[aD(\omega)]_{mn} = \sum_{l=-\infty}^{\infty} [a]_{ml}[D(\omega)]_{ln}. \tag{A·5}$$

By substituting Eqs. (44) and (50) into Eqs. (A·2) and (A·3), respectively, and using the Floquet representation and these relations, we obtain

$$\begin{aligned}
\sigma^{\mathrm{Q}(1)}_{yx}(\omega) &= \int_0^{T_{\mathrm{p}}} \frac{dt_{\mathrm{av}}}{T_{\mathrm{p}}} \int_{-\infty}^{\infty} dt_{\mathrm{rel}}\, e^{i\omega t_{\mathrm{rel}}} \sigma^{\mathrm{Q}(1)}_{yx}\left(t_{\mathrm{av}} + \frac{t_{\mathrm{rel}}}{2}, t_{\mathrm{av}} - \frac{t_{\mathrm{rel}}}{2}\right) \\
&= -\frac{1}{\omega N} \sum_{\mathbf{k}} \sum_{a,b} \sum_{\sigma} \int_{-\Omega/2}^{\Omega/2} \frac{d\omega'}{2\pi} \sum_{m,l=-\infty}^{\infty} [M^{(\mathrm{Q})yx}_{ab\sigma}(\mathbf{k})]_{ml}[G^{<}_{b\sigma a\sigma}(\mathbf{k},\omega')]_{lm} \\
&= -\frac{1}{\omega N} \sum_{\mathbf{k}} \sum_{a,b} \sum_{\sigma} \int_{-\Omega/2}^{\Omega/2} \frac{d\omega'}{2\pi} \mathrm{tr}[M^{(\mathrm{Q})yx}_{ab\sigma}(\mathbf{k}) G^{<}_{b\sigma a\sigma}(\mathbf{k},\omega')],
\end{aligned} \tag{A·6}$$

$$\begin{aligned}
\sigma^{\mathrm{Q}(2)}_{yx}(\omega) &= \int_0^{T_{\mathrm{p}}} \frac{dt_{\mathrm{av}}}{T_{\mathrm{p}}} \int_{-\infty}^{\infty} dt_{\mathrm{rel}}\, e^{i\omega t_{\mathrm{rel}}} \sigma^{\mathrm{Q}(2)}_{yx}\left(t_{\mathrm{av}} + \frac{t_{\mathrm{rel}}}{2}, t_{\mathrm{av}} - \frac{t_{\mathrm{rel}}}{2}\right) \\
&= \frac{1}{\omega N} \sum_{\mathbf{k}} \sum_{a,b,c,d} \sum_{\sigma,\sigma'} \int_{-\Omega/2}^{\Omega/2} \frac{d\omega'}{2\pi} \sum_{m,n,l,q=-\infty}^{\infty} \\
&\quad \times \{[v^{(\mathrm{Q})y}_{ab\sigma}(\mathbf{k})]_{ml}[G^{\mathrm{R}}_{b\sigma c\sigma'}(\mathbf{k},\omega'+\omega)]_{ln}[v^{(\mathrm{C})x}_{cd\sigma'}(\mathbf{k})]_{nq}[G^{<}_{d\sigma' a\sigma}(\mathbf{k},\omega')]_{qm} \\
&\quad + [v^{(\mathrm{Q})y}_{ab\sigma}(\mathbf{k})]_{ml}[G^{<}_{b\sigma c\sigma'}(\mathbf{k},\omega')]_{ln}[v^{(\mathrm{C})x}_{cd\sigma'}(\mathbf{k})]_{nq}[G^{\mathrm{A}}_{d\sigma' a\sigma}(\mathbf{k},\omega'-\omega)]_{qm}\} \\
&= \frac{1}{\omega N} \sum_{\mathbf{k}} \sum_{a,b,c,d} \sum_{\sigma,\sigma'} \int_{-\Omega/2}^{\Omega/2} \frac{d\omega'}{2\pi} \{\mathrm{tr}[v^{(\mathrm{Q})y}_{ab\sigma}(\mathbf{k}) G^{\mathrm{R}}_{b\sigma c\sigma'}(\mathbf{k},\omega'+\omega) v^{(\mathrm{C})x}_{cd\sigma'}(\mathbf{k}) G^{<}_{d\sigma' a\sigma}(\mathbf{k},\omega')] \\
&\quad + \mathrm{tr}[v^{(\mathrm{Q})y}_{ab\sigma}(\mathbf{k}) G^{<}_{b\sigma c\sigma'}(\mathbf{k},\omega') v^{(\mathrm{C})x}_{cd\sigma'}(\mathbf{k}) G^{\mathrm{A}}_{d\sigma' a\sigma}(\mathbf{k},\omega'-\omega)]\},
\end{aligned} \tag{A·7}$$

where

$$[M^{(\mathrm{Q})yx}_{ab\sigma}(\mathbf{k})]_{ml} = \int_0^{T_\mathrm{p}} \frac{dt}{T_\mathrm{p}} e^{i(m-l)\Omega t} \frac{\delta v^{(\mathrm{Q})y}_{ab\sigma}(\mathbf{k},t)}{\delta A^x_{\mathrm{prob}}(t)}. \tag{A·8}$$

Since $\sigma^{\mathrm{Q}(1)}_{yx}(\omega)$ has only a pure imaginary part,[49] we have

$$\sigma^{\mathrm{Q}}_{yx}(\omega) = \frac{1}{\omega N}\sum_{\mathbf{k}}\sum_{a,b,c,d}\sum_{\sigma,\sigma'}\int_{-\Omega/2}^{\Omega/2}\frac{d\omega'}{2\pi}\mathrm{Re}\{\mathrm{tr}[v^{(\mathrm{Q})y}_{ab\sigma}(\mathbf{k})G^{\mathrm{R}}_{b\sigma c\sigma'}(\mathbf{k},\omega'+\omega)v^{(\mathrm{C})x}_{cd\sigma'}(\mathbf{k})G^{<}_{d\sigma' a\sigma}(\mathbf{k},\omega')]$$
$$+\mathrm{tr}[v^{(\mathrm{Q})y}_{ab\sigma}(\mathbf{k})G^{<}_{b\sigma c\sigma'}(\mathbf{k},\omega')v^{(\mathrm{C})x}_{cd\sigma'}(\mathbf{k})G^{\mathrm{A}}_{d\sigma' a\sigma}(\mathbf{k},\omega'-\omega)]\}. \tag{A·9}$$

Moreover, we can rewrite this expression by using the identity,

$$\mathrm{Re}[\mathrm{tr}(AB)] = \frac{1}{2}\{\mathrm{tr}(AB)+\mathrm{tr}[(AB)^\dagger]\}, \tag{A·10}$$

and the symmetry relations of quantities in the Floquet representation,

$$[G^{<}_{d\sigma' a\sigma}(\mathbf{k},\omega')^\dagger]_{ml} = -[G^{<}_{a\sigma d\sigma'}(\mathbf{k},\omega')]_{ml}, \tag{A·11}$$
$$[v^{(\mathrm{C})x}_{cd\sigma'}(\mathbf{k})^\dagger]_{ln} = [v^{(\mathrm{C})x}_{dc\sigma'}(\mathbf{k})]_{ln}, \tag{A·12}$$
$$[G^{\mathrm{R}}_{b\sigma c\sigma'}(\mathbf{k},\omega'+\omega)^\dagger]_{nq} = [G^{\mathrm{A}}_{c\sigma' b\sigma}(\mathbf{k},\omega'+\omega)]_{nq}, \tag{A·13}$$
$$[v^{(\mathrm{Q})y}_{ab\sigma}(\mathbf{k})^\dagger]_{qm} = [v^{(\mathrm{Q})y}_{ba\sigma}(\mathbf{k})]_{qm}. \tag{A·14}$$

Note that Eqs. (A·11) and (A·13) are obtained by using

$$G^{<}_{d\sigma' a\sigma}\left(\mathbf{k};t_{\mathrm{av}}+\frac{t_{\mathrm{rel}}}{2},t_{\mathrm{av}}-\frac{t_{\mathrm{rel}}}{2}\right)^\dagger = -G^{<}_{a\sigma d\sigma'}\left(\mathbf{k};t_{\mathrm{av}}-\frac{t_{\mathrm{rel}}}{2},t_{\mathrm{av}}+\frac{t_{\mathrm{rel}}}{2}\right), \tag{A·15}$$

and

$$G^{\mathrm{R}}_{b\sigma c\sigma'}\left(\mathbf{k};t_{\mathrm{av}}+\frac{t_{\mathrm{rel}}}{2},t_{\mathrm{av}}-\frac{t_{\mathrm{rel}}}{2}\right)^\dagger = G^{\mathrm{A}}_{c\sigma' b\sigma}\left(\mathbf{k};t_{\mathrm{av}}-\frac{t_{\mathrm{rel}}}{2},t_{\mathrm{av}}+\frac{t_{\mathrm{rel}}}{2}\right), \tag{A·16}$$

respectively. Using Eqs. (A·10)–(A·14), we obtain

$$\frac{1}{\omega}\mathrm{Re}\{\mathrm{tr}[v^{(\mathrm{Q})y}_{ab\sigma}(\mathbf{k})G^{\mathrm{R}}_{b\sigma c\sigma'}(\mathbf{k},\omega'+\omega)v^{(\mathrm{C})x}_{cd\sigma'}(\mathbf{k})G^{<}_{d\sigma' a\sigma}(\mathbf{k},\omega')]\}$$
$$=\frac{1}{2\omega}\{\mathrm{tr}[v^{(\mathrm{Q})y}_{ab\sigma}(\mathbf{k})G^{\mathrm{R}}_{b\sigma c\sigma'}(\mathbf{k},\omega'+\omega)v^{(\mathrm{C})x}_{cd\sigma'}(\mathbf{k})G^{<}_{d\sigma' a\sigma}(\mathbf{k},\omega')]$$
$$-\mathrm{tr}[G^{<}_{a\sigma d\sigma'}(\mathbf{k},\omega')v^{(\mathrm{C})x}_{dc\sigma'}(\mathbf{k})G^{\mathrm{A}}_{c\sigma' b\sigma}(\mathbf{k},\omega'+\omega)v^{(\mathrm{Q})y}_{ba\sigma}(\mathbf{k})]\}, \tag{A·17}$$

and

$$\frac{1}{\omega}\mathrm{Re}\{\mathrm{tr}[v^{(\mathrm{Q})y}_{ab\sigma}(\mathbf{k})G^{<}_{b\sigma c\sigma'}(\mathbf{k},\omega')v^{(\mathrm{C})x}_{cd\sigma'}(\mathbf{k})G^{\mathrm{A}}_{d\sigma' a\sigma}(\mathbf{k},\omega'-\omega)]\}$$
$$=\frac{1}{2\omega}\{\mathrm{tr}[v^{(\mathrm{Q})y}_{ab\sigma}(\mathbf{k})G^{<}_{b\sigma c\sigma'}(\mathbf{k},\omega')v^{(\mathrm{C})x}_{cd\sigma'}(\mathbf{k})G^{\mathrm{A}}_{d\sigma' a\sigma}(\mathbf{k},\omega'-\omega)]$$
$$-\mathrm{tr}[G^{\mathrm{R}}_{a\sigma d\sigma'}(\mathbf{k},\omega'-\omega)v^{(\mathrm{C})x}_{dc\sigma'}(\mathbf{k})G^{<}_{c\sigma' b\sigma}(\mathbf{k},\omega')v^{(\mathrm{Q})y}_{ba\sigma}(\mathbf{k})]\}. \tag{A·18}$$

Substituting Eqs. (A·17) and (A·18) into Eq. (A·9), we obtain Eq. (55).

Appendix B: $[\epsilon_{ab}(\mathbf{k})]_{mn}$ of Sr_2RuO_4 Driven by BCPL

We can calculate $[\epsilon_{ab}(\mathbf{k})]_{mn}$ of Sr_2RuO_4 driven by BCPL by using Eqs. (12) and (13) and Eq. (73). To do this, we use identities,

$$e^{iu\sin(\Omega t+\theta)} = \sum_{l=-\infty}^{\infty}\mathcal{J}_l(u)e^{il(\Omega t+\theta)}, \tag{B·1}$$

$$e^{iu\cos(\Omega t+\theta)} = \sum_{l=-\infty}^{\infty} i^l\mathcal{J}_l(u)e^{il(\Omega t+\theta)}, \tag{B·2}$$

$$\mathcal{J}_l(u) = (-1)^l\mathcal{J}_l(-u) = (-1)^l\mathcal{J}_{-l}(u), \tag{B·3}$$

where $\mathcal{J}_l(u)$ is the Bessel function of the first kind, and l is its order. After some calculation, we obtain

$$[\epsilon_{d_{yz}d_{yz}}(\mathbf{k})]_{mn} = (-t_2)\sum_{l=-\infty}^{\infty} i^{n-m-(\beta-1)l}e^{-il\theta}\mathcal{J}_{n-m-\beta l}(u)\mathcal{J}_l(u)[e^{-ik_x}(-1)^{n-m-(\beta-1)l}+e^{ik_x}]$$

$$+(-t_1)\sum_{l=-\infty}^{\infty} e^{-il\theta}(-1)^l \mathcal{J}_{n-m-\beta l}(u)\mathcal{J}_l(u)[e^{-ik_y}(-1)^{n-m-(\beta-1)l}+e^{ik_y}], \tag{B·4}$$

$$[\epsilon_{d_{zx}d_{zx}}(\mathbf{k})]_{mn} = (-t_1)\sum_{l=-\infty}^{\infty} i^{n-m-(\beta-1)l} e^{-il\theta}\mathcal{J}_{n-m-\beta l}(u)\mathcal{J}_l(u)[e^{-ik_x}(-1)^{n-m-(\beta-1)l}+e^{ik_x}]$$
$$+(-t_2)\sum_{l=-\infty}^{\infty} e^{-il\theta}(-1)^l \mathcal{J}_{n-m-\beta l}(u)\mathcal{J}_l(u)[e^{-ik_y}(-1)^{n-m-(\beta-1)l}+e^{ik_y}], \tag{B·5}$$

$$[\epsilon_{d_{yz}d_{zx}}(\mathbf{k})]_{mn} = [\epsilon_{d_{zx}d_{yz}}(\mathbf{k})]_{mn} = t_5\sum_{l,l',l''=-\infty}^{\infty} i^{l+l'}e^{-i(l'+l'')\theta}\mathcal{J}_l(u)\mathcal{J}_{l'}(u)\mathcal{J}_{n-m-l-(l'+l'')\beta}(u)\mathcal{J}_{l''}(u)$$
$$\times[e^{-ik_x}e^{-ik_y}(-1)^{n-m-(l'+l'')\beta+l'}+e^{ik_x}e^{ik_y}(-1)^{l''}$$
$$-e^{-ik_x}e^{ik_y}(-1)^{l+l'+l''}-e^{ik_x}e^{-ik_y}(-1)^{n-m-l-(l'+l'')\beta}], \tag{B·6}$$

$$[\epsilon_{d_{xy}d_{xy}}(\mathbf{k})]_{mn} = (-t_3)\sum_{l=-\infty}^{\infty} e^{-il\theta}\mathcal{J}_{n-m-\beta l}(u)\mathcal{J}_l(u)[i^{n-m-(\beta-1)l}e^{-ik_x}(-1)^{n-m-(\beta-1)l}+i^{n-m-(\beta-1)l}e^{ik_x}$$
$$+e^{-ik_y}(-1)^{n-m-\beta l}+e^{ik_y}(-1)^l]$$
$$+(-t_4)\sum_{l,l',l''=-\infty}^{\infty} i^{l+l'}e^{-i(l'+l'')\theta}\mathcal{J}_l(u)\mathcal{J}_{l'}(u)\mathcal{J}_{n-m-l-(l'+l'')\beta}(u)\mathcal{J}_{l''}(u)$$
$$\times[e^{-ik_x}e^{-ik_y}(-1)^{n-m-(l'+l'')\beta+l'}+e^{ik_x}e^{ik_y}(-1)^{l''}+e^{-ik_x}e^{ik_y}(-1)^{l+l'+l''}$$
$$+e^{ik_x}e^{-ik_y}(-1)^{n-m-l-(l'+l'')\beta}], \tag{B·7}$$

where

$$u = ea_{\mathrm{NN}}A_0 = eA_0. \tag{B·8}$$

As described in Sect. 3, t_1, t_2, and t_3 are the nearest-neighbor hopping integrals on the square lattice, and t_4 and t_5 are the next-nearest-neighbor ones[11] [Fig. 5(a)].

We make three comments about Eqs. (B·4)–(B·7). First, the relative phase difference in BCPL, θ, causes the phase factors, such as $e^{-il\theta}$ and $e^{-i(l'+l'')\theta}$, only for the terms of the finite-order Bessel functions. Second, the number of the Bessel functions is twice that in the case of CPL.[11] This is because the x or y component of the pump field contains two trigonometric functions in the case of BCPL, whereas it contains one in the case of CPL.[11] Third, even if the Floquet indices m, n, l, l', and l'' are restricted to the range of $-n_{\max} \le m, n, l, l', l'' \le n_{\max}$, $[\epsilon_{ab}(\mathbf{k})]_{mn}$'s include not only the Bessel functions the order of which is within this range, but also the Bessel functions the order of which is outside of it. For example, if $\beta = 2$ and $-1 \le m, n, l \le 1$ (i.e., $n_{\max} = 1$), the order of the first Bessel function in Eq. (B·4), $\mathcal{J}_{n-m-\beta l}(u)$, takes the value outside of that range. Since the third property is also related to the number of the trigonometric functions appearing in the Peierls phase factors, this suggests that the high-order Bessel functions play a more important role in the case of BCPL than in that of CPL. In fact, this is consistent with the difference between the $n_{\max}$ dependences of σ^{S}_{yx} obtained for BCPL and CPL.

Appendix C: $[\bar{\epsilon}_{ab}(\mathbf{k})]_{mn}$ of Sr_2RuO_4 Driven by BCPL

We can calculate $[\bar{\epsilon}_{ab}(\mathbf{k})]_{mn}$ of Sr_2RuO_4 driven by BCPL in a similar way to the calculation explained in Appendix B. After such calculation using Eqs. (15), (16), and (85), we obtain

$$[\bar{\epsilon}_{d_{yz}d_{yz}}(\mathbf{k})]_{mn} = (-t_2)\sum_{l=-\infty}^{\infty} i^{n-m-(\beta-1)l}e^{il\theta}\mathcal{J}_{n-m-\beta l}(u)\mathcal{J}_l(u)[e^{-ik_x}(-1)^{n-m-(\beta-1)l}+e^{ik_x}]$$
$$+(-t_1)\sum_{l=-\infty}^{\infty} e^{il\theta}(-1)^{n-m-\beta l}\mathcal{J}_{n-m-\beta l}(u)\mathcal{J}_l(u)[e^{-ik_y}(-1)^{n-m-(\beta-1)l}+e^{ik_y}], \tag{C·1}$$

$$[\bar{\epsilon}_{d_{zx}d_{zx}}(\mathbf{k})]_{mn} = (-t_1)\sum_{l=-\infty}^{\infty} i^{n-m-(\beta-1)l}e^{il\theta}\mathcal{J}_{n-m-\beta l}(u)\mathcal{J}_l(u)[e^{-ik_x}(-1)^{n-m-(\beta-1)l}+e^{ik_x}]$$
$$+(-t_2)\sum_{l=-\infty}^{\infty} e^{il\theta}(-1)^{n-m-\beta l}\mathcal{J}_{n-m-\beta l}(u)\mathcal{J}_l(u)[e^{-ik_y}(-1)^{n-m-(\beta-1)l}+e^{ik_y}], \tag{C·2}$$

$$[\bar{\epsilon}_{d_{yz}d_{zx}}(\mathbf{k})]_{mn} = [\bar{\epsilon}_{d_{zx}d_{yz}}(\mathbf{k})]_{mn} = t_5\sum_{l,l',l''=-\infty}^{\infty} i^{l+l'}e^{i(l'+l'')\theta}\mathcal{J}_l(u)\mathcal{J}_{l'}(u)\mathcal{J}_{n-m-l-(l'+l'')\beta}(u)\mathcal{J}_{l''}(u)$$
$$\times[e^{-ik_x}e^{-ik_y}(-1)^{l+l'+l''}+e^{ik_x}e^{ik_y}(-1)^{n-m-l-(l'+l'')\beta}-e^{-ik_x}e^{ik_y}(-1)^{n-m-(l'+l'')\beta+l'}$$
$$-e^{ik_x}e^{-ik_y}(-1)^{l''}], \tag{C·3}$$

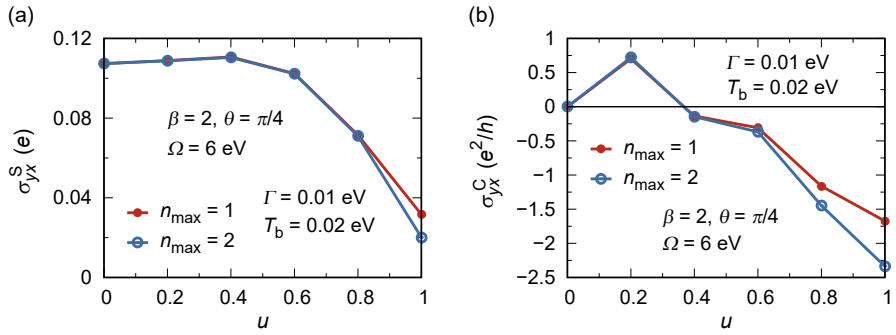

Fig. D·1. (Color online) The $n_{\max}$ dependences of (a) σ^{S}_{yx} and (b) σ^{C}_{yx} as functions of u ($= eA_0$) for Sr_2RuO_4 driven by BCPL at $\beta = 2$, $\theta = \frac{\pi}{4}$, and $\Omega = 6$ eV. Here $n_{\max}$ is the upper limit of the summation over the Floquet indices. The values of $N_x = N_y$ and $\Delta\omega'$ used in their numerical calculations are different from those used in the numerical calculations for the results shown in Sect. 5: $N_x = N_y = 64$ and $\Delta\omega' = 0.01$ eV were used in the former calculations, whereas $N_x = N_y = 100$ and $\Delta\omega' = 0.005$ eV were used in the latter calculations. Meanwhile, the values of Γ and T_b are the same.

$$
\begin{aligned}
[\bar{\epsilon}_{d_{xy}d_{xy}}(\mathbf{k})]_{mn} = (-t_3) \sum_{l=-\infty}^{\infty} e^{il\theta} \mathcal{J}_{n-m-\beta l}(u)\mathcal{J}_l(u)[i^{n-m-(\beta-1)l}e^{-ik_x}(-1)^{n-m-(\beta-1)l} + i^{n-m-(\beta-1)l}e^{ik_x} \\
+ e^{-ik_y}(-1)^l + e^{ik_y}(-1)^{n-m-\beta l}] \\
+ (-t_4) \sum_{l,l',l''=-\infty}^{\infty} i^{l+l'} e^{i(l'+l'')\theta} \mathcal{J}_l(u)\mathcal{J}_{l'}(u)\mathcal{J}_{n-m-l-(l'+l'')\beta}(u)\mathcal{J}_{l''}(u) \\
\times [e^{-ik_x}e^{-ik_y}(-1)^{l+l'+l''} + e^{ik_x}e^{ik_y}(-1)^{n-m-l-(l'+l'')\beta} + e^{-ik_x}e^{ik_y}(-1)^{n-m-(l'+l'')\beta+l'} \\
+ e^{ik_x}e^{-ik_y}(-1)^{l''}].
\end{aligned}
\tag{C·4}
$$

These equations and Eqs. (B·4)–(B·7) show that the differences between $[\bar{\epsilon}_{ab}(\mathbf{k})]_{mn}$'s and $[\epsilon_{ab}(\mathbf{k})]_{mn}$'s are the differences in the phase factors due to θ and the sign factors such as $(-1)^l$ and $(-1)^{n-m-\beta l}$. These differences are reasonable because $\mathbf{A}_{\mathrm{BCPL}}(-t)$ and $\mathbf{A}_{\mathrm{BCPL}}(t)$ are given by Eqs. (15) and (16) and by Eqs. (12) and (13), respectively.

Appendix D: Additional Numerical Results

We show additional numerical results to discuss the validity of our choice of the value of $n_{\max}$. Figures D·1(a) and D·1(b) show the $n_{\max}$ dependences of σ^{S}_{yx} and σ^{C}_{yx} for Sr_2RuO_4 driven by BCPL at $\beta = 2$, $\theta = \frac{\pi}{4}$, and $\Omega = 6$ eV. In obtaining these results, we chose some parameters to be different from the values used in the numerical results shown in Sect. 5: we set $N_x = N_y = 64$ and $\Delta\omega' = 0.01$ eV to reduce the cost of the numerical calculations. These figures show that the results obtained for $n_{\max} = 1$ and 2 are qualitatively the same. Therefore, $n_{\max} = 1$ may be reasonable to study qualitative properties of σ^{S}_{yx} and σ^{C}_{yx} for Sr_2RuO_4 driven by BCPL at $\Omega = 6$ eV.

*arakawa@phys.chuo-u.ac.jp

1) J. H. Shirley, Phys. Rev. **138**, B979 (1965).
2) H. Sambe, Phys. Rev. A **7**, 2203 (1973).
3) M. Bukov, L. D'Alessio, and A. Polkovnikov, Adv. Phys. **64**, 139 (2015).
4) A. Eckardt, Rev. Mod. Phys. **89**, 011004 (2017).
5) T. Oka and S. Kitamura, Annu. Rev. Condens. Matter Phys. **10**, 387 (2019).
6) N. Arakawa and K. Yonemitsu, Phys. Rev. B **103**, L100408 (2021).
7) T. Oka and H. Aoki, Phys. Rev. B **79**, 081406(R) (2009).
8) T. Mikami, S. Kitamura, K. Yasuda, N. Tsuji, T. Oka, and H. Aoki, Phys. Rev. B **93**, 144307 (2016).
9) C. M. Yin, N. Tang, S. Zhang, J. X. Duan, F. J. Xu, J. Song, F. H. Mei, X. Q. Wang, B. Shen, Y. H. Chen, J. L. Yu, and H. Ma, Appl. Phys. Lett. **98**, 122104 (2011).
10) J. W. McIver, B. Schulte, F.-U. Stein, T. Matsuyama, G. Jotzu, G. Meier, and A. Cavalleri, Nat. Phys. **16**, 38 (2020).
11) N. Arakawa and K. Yonemitsu, Commun. Phys. **6**, 43 (2023).
12) E. H. Hall, Philos. Mag. **12**, 157 (1881).
13) R. Karplus and J. M. Luttinger, Phys. Rev. **95**, 1154 (1954).
14) N. Nagaosa, J. Sinova, S. Onoda, A. H. MacDonald, and N. P. Ong, Rev. Mod. Phys. **82**, 1539 (2010).
15) N. Arakawa and K. Yonemitsu, Phys. Rev. B **111**, L121110 (2025).
16) M. I. D'yakonov and V. I. Perel', ZhETF Pis. Red. **13**, 657 (1971) [Sov. Phys. JETP Lett. **13**, 467 (1971)].
17) J. E. Hirsch, Phys. Rev. Lett. **83**, 1834 (1999).
18) J. Sinova, S. O. Valenzuela, J. Wunderlich, C. H. Back, and T. Jungwirth, Rev. Mod. Phys. **87**, 1213 (2015).
19) L. Onsager, Phys. Rev. **37**, 405 (1931).
20) L. Onsager, Phys. Rev. **38**, 2265 (1931).
21) R. Kubo, J. Phys. Soc. Jpn. **12**, 570 (1957).
22) E. Saitoh, M. Ueda, H. Miyajima, and G. Tatara, Appl. Phys. Lett. **88**, 182509 (2006).
23) S. O. Valenzuela and M. Tinkham, Nature **442**, 176 (2006).
24) K. Brandner, K. Saito, and U. Seifert, Phys. Rev. X **5**, 031019 (2015).
25) K. Proesmans and C. Van den Broeck, Phys. Rev. Lett. **115**, 090601 (2015).
26) E. Potanina, C. Flindt, M. Moskalets, and K. Brandner, Phys. Rev. X **11**, 021013 (2021).
27) N. Arakawa and K. Yonemitsu, J. Phys. Soc. Jpn. **93**, 084701 (2024).
28) O. Kfir, P. Grychtol, E. Turgut, R. Knut, D. Zusin, D. Popmintchev, T. Popmintchev, H. Nembach, J. M. Shaw, A. Fleischer, H. Kapteyn, M. Murnane, and O. Cohen, Nat. Photonics **9**, 99 (2015).
29) T. Nag, R.-J. Slager, T. Higuchi, and T. Oka, Phys. Rev. B **100**, 134301 (2019).
30) N. Arakawa and K. Yonemitsu, Phys. Rev. B **109**, L241201 (2024).
31) Y. H. Wang, H. Steinberg, P. Jarillo-Herrero, and N. Gedik, Science **342**, 453 (2013).
32) N. Arakawa, Phys. Rev. B **105**, 174303 (2022).
33) N. Arakawa, Phys. Rev. B **106**, 064306 (2022).
34) J. Shi, P. Zhang, D. Xiao, and Q. Niu, Phys. Rev. Lett. **96**, 076604 (2006).
35) T. Kimura, Y. Otani, T. Sato, S. Takahashi, and S. Maekawa, Phys.

Rev. Lett. **98**, 156601 (2007).
36) Q.-f. Sun, X. C. Xie, and J. Wang, Phys. Rev. B **77**, 035327 (2008).
37) H. Pan, Z. Liu, D. Hou, Y. Gao, and Q. Niu, Phys. Rev. Res. **6**, L012034 (2024).
38) N. Tsuji, T. Oka, and H. Aoki, Phys. Rev. Lett. **103**, 047403 (2009).
39) L. D'Alessio and M. Rigol, Phys. Rev. X **4**, 041048 (2014).
40) A. Lazarides, A. Das, and R. Moessner, Phys. Rev. E **90**, 012110 (2014).
41) N. Arakawa and M. Ogata, Phys. Rev. B **87**, 195110 (2013).
42) N. Arakawa, Phys. Rev. B **90**, 245103 (2014).
43) T. Oguchi, J. Phys. Soc. Jpn. **78**, 044702 (2009).
44) A. Damascelli, D. H. Lu, K. M. Shen, N. P. Armitage, F. Ronning, D. L. Feng, C. Kim, Z.-X. Shen, T. Kimura, Y. Tokura, Z. Q. Mao, and Y. Maeno, Phys. Rev. Lett. **85**, 5194 (2000).
45) H. Kontani, T. Tanaka, D. S. Hirashima, K. Yamada, and J. Inoue, Phys. Rev. Lett. **100**, 096601 (2008).
46) T. Mizoguchi and N. Arakawa, Phys. Rev. B **93**, 041304(R) (2016).
47) M. Büttiker, Phys. Rev. B **32**, 1846(R) (1985).
48) M. Büttiker, Phys. Rev. B **33**, 3020 (1986).
49) M. Eckstein and M. Kollar, Phys. Rev. B **78**, 205119 (2008).
50) A. Kirilyuk, A. V. Kimel, and T. Rasing, Rev. Mod. Phys. **82**, 2731 (2010).
51) G. D. Mahan, *Many-Particle Physics* (Plenum, New York, 2000).
52) L. V. Keldysh, Zh. Eksp. Teor. Fiz. **47**, 1515 (1964) [Sov. Phys. JETP **20**, 1018 (1965)].
53) L. P. Kadanoff and G. Baym, *Quantum Statistical Mechanics* (Perseus Books, New York, 1989).
54) J. Maciejko, *An Introduction to Nonequilibrium Many-Body Theory* (Springer, Berlin, 2007).
55) D. C. Langreth and J. W. Wilkins, Phys. Rev. B **6**, 3189 (1972).
56) N. Tsuji, T. Oka, and H. Aoki, Phys. Rev. B **78**, 235124 (2008).
57) A. I. Larkin and Yu. N. Ovchinnikov, Zh. Eksp. Teor. Fiz. **68**, 1915 (1975) [Sov. Phys. JETP **41**, 960 (1976)].
58) A. Eckardt and E. Anisimovas, New J. Phys. **17**, 093039 (2015).
59) T. Kitagawa, T. Oka, A. Brataas, L. Fu, and E. Demler, Phys. Rev. B **84**, 235108 (2011).
60) H. Kontani, T. Tanaka, and K. Yamada, Phys. Rev. B **75**, 184416 (2007).
61) T. Tanaka, H. Kontani, M. Naito, T. Naito, D. S. Hirashima, K. Yamada, and J. Inoue, Phys. Rev. B **77**, 165117 (2008).
62) N. Arakawa, Phys. Rev. B **93**, 245128 (2016).
63) P. Streda, J. Phys. C **15**, L717 (1982).
64) D. J. Thouless, M. Kohmoto, M. P. Nightingale, and M. den Nijs, Phys. Rev. Lett. **49**, 405 (1982).
65) H. Fukuyama, H. Ebisawa, and Y. Wada, Prog. Theor. Phys. **42**, 494 (1969).
66) Y. Zhang, J. Li, L. Li, T. Huang, X. Zhu, P. Lan, and P. Lu, Opt. Express **29**, 17387 (2021).
67) R. Habara and K. Wakabayashi, Phys. Rev. B **107**, 115422 (2023).
68) Y. Ikeda, S. Kitamura, and T. Morimoto, Phys. Rev. Lett. **131**, 096301 (2023).
69) M. A. Nichols, L. W. Cheuk, M. Okan, T. R. Hartke, E. Mendez, T. Senthil, E. Khatami, H. Zhang, and M. W. Zwierlein, Science **363**, 383 (2019).
70) O. Chmaissem, J. D. Jorgensen, H. Shaked, S. Ikeda, and Y. Maeno, Phys. Rev. B **57**, 5067 (1998).
71) Y. Kawakami, H. Itoh, K. Yonemitsu, and S. Iwai, J. Phys. B **51**, 174005 (2018).
72) G. E. W. Bauer, E. Saitoh, and B. J. van Wees, Nat. Mater. **11**, 391 (2012).
73) K. Uchida, S. Takahashi, K. Harii, J. Ieda, W. Koshibae, K. Ando, S. Maekawa, and E. Saitoh, Nature **455**, 778 (2008).
74) K. Uchida, J. Xiao, H. Adachi, J. Ohe, S. Takahashi, J. Ieda, T. Ota, Y. Kajiwara, H. Umezawa, H. Kawai, G. E. W. Bauer, S. Maekawa, and E. Saitoh, Nat. Mater. **9**, 894 (2010).
75) H. Adachi, K. Uchida, E. Saitoh, and S. Maekawa, Rep. Prog. Phys. **76**, 036501 (2013).